

Contract No. W-7405-eng-26

Reactor Division

SOLUTION OF THE EQUATION DESCRIBING THE INTERFACE BETWEEN TWO  
FLUIDS FOR THE VOLUME AND PRESSURE WITHIN ATTACHED,  
SESSILE SHAPED, BUBBLES AND DROPS

J. W. Cooke

AUGUST 1971

This report was prepared as an account of work sponsored by the United States Government. Neither the United States nor the United States Atomic Energy Commission, nor any of their employees, nor any of their contractors, subcontractors, or their employees, makes any warranty, express or implied, or assumes any legal liability or responsibility for the accuracy, completeness or usefulness of any information, apparatus, product or process disclosed, or represents that its use would not infringe privately owned rights.

OAK RIDGE NATIONAL LABORATORY  
Oak Ridge, Tennessee  
Operated by  
UNION CARBIDE CORPORATION  
for the  
U. S. ATOMIC ENERGY COMMISSION

10

10

10

## CONTENTS

	<u>Page</u>
Abstract . . . . .	1
Introduction . . . . .	1
Derivation of the Interfacial Equation . . . . .	2
Numerical Solution of the Interfacial Equation . . . . .	5
Computer Program . . . . .	7
Solution of the Differential Equation . . . . .	7
Solution for $h/a$ and $V/a^3$ versus $\beta$ and $\phi$ . . . . .	7
Solution for $h/a$ and $V/a^3$ versus $\beta$ and $r/a$ . . . . .	8
Solution for $\bar{h}/a$ and $\bar{V}/a^3$ versus $r/a$ . . . . .	8
Range, Running Time, and Accuracy . . . . .	10
Results . . . . .	10
Discussion of Results . . . . .	17
Estimation of the Accuracy . . . . .	17
Comparison with Previous Results . . . . .	17
Conclusions . . . . .	21
References . . . . .	21
Nomenclature . . . . .	22
Appendices . . . . .	25
A. Parametric Crossplots . . . . .	27
B. Tabulated Results . . . . .	33
C. Computer Program . . . . .	43

.)

.

.)

SOLUTION OF THE EQUATION DESCRIBING THE INTERFACE BETWEEN TWO  
FLUIDS FOR THE VOLUME AND PRESSURE WITHIN ATTACHED,  
SESSILE SHAPED, BUBBLES AND DROPS

J. W. Cooke

ABSTRACT

A numerical computer program was written to solve the equation describing the interface between two immiscible fluids to obtain the shape, size, volume, and pressure of attached bubbles and droplets. These relationships are important to the study of three-phase heat transfer, superheat, critical constants, and interfacial energies. Previous solutions have been obtained with limited accuracy for a restricted number and range of variables. The present results are given in both graphical and tabular form for a wide range and number of parameters, and the computer program is included so that an even broader range and number of variables, as well as specific values, can be obtained as required. In particular, an expression for the maximum-bubble-pressure was derived which is considerably more accurate over a wider range than previous expressions.

Keywords. Surface tension, interfacial tension, bubbles, drops, contact angle, maximum-bubble-pressure, fluid-vapor interface.

---

INTRODUCTION

A knowledge of relationships among volume, pressure, shape, and size of attached bubbles and droplets are important in the study of boiling and condensing heat transfer, superheat and critical point phenomena, mass transfer studies, and in the measurement of contact angles and surface tension.<sup>1-4</sup> These relationships can be obtained from the solution of the second-order, nonlinear differential equation describing the interface between two fluids. This equation has been solved by perturbation analysis for very small bubble sizes by Rayleigh<sup>5</sup> and Schrödinger,<sup>6</sup> by numerical hand calculations for a wide range of discrete drop shapes by Bashforth and Adams,<sup>7</sup> and by numerical computer calculations for droplet volumes and heights by Baumeister and Hamill.<sup>8</sup> However, the Rayleigh-Schrödinger solution is no longer used extensively because of concern regarding its accuracy; and the Bashforth and Adams (as well as the

Baumeister and Hamill) solutions were obtained for a limited number and range of variables.

In order to check the accuracy and to extend the usefulness of the above solutions, a numerical computer program was written to solve the interfacial equation. The subject program solves the interfacial equation for any value of the dimensionless shape parameter,  $\beta$ , for positive values of the term  $\beta Z$  (sessile drops or above-attached bubbles)\* and extends the previous solutions for  $\phi > 180$  degrees. The solution not only provides the dimensionless  $X$ ,  $Z$ ,  $\phi$  coordinates describing the profiles of the interface, but also gives the bubble volume within and the pressure difference across the interface as a function of profile shape and, in addition, the maximum pressure difference across the interface for a given radius of attachment (which is required for the calculation of the surface tension by the maximum-bubble-pressure technique).

This report describes the derivation of the interfacial equation, its numerical solution, and the computer program employed. The results and an estimation of their accuracy are presented and compared with the previous solutions.

#### DERIVATION OF THE INTERFACIAL EQUATION

At the interface separating two immiscible fluids (usually a liquid and its vapor), a force imbalance exists which results in an interfacial tension. The tension is a force per unit length pulling uniformly in all directions tangent to the interface. Neglecting gravitational forces, a force balance on an infinitesimal segment of a free surface is shown in Fig. 1-a. The surface is bowed by a uniform differential pressure,  $P$ , where  $r_1$  and  $r_2$  are the principal radii of curvature. The force balance would thus be:

$$P \Delta x \Delta z = 2\gamma \left( \Delta x \frac{\Delta z}{2r_1} + \Delta z \frac{\Delta x}{2r_2} \right), \quad (1)$$

---

\*The case for negative values of the term  $\beta Z$  (pendant drops or below-attached bubbles) will be presented in a later report.

ORNL-DWG 71-7609

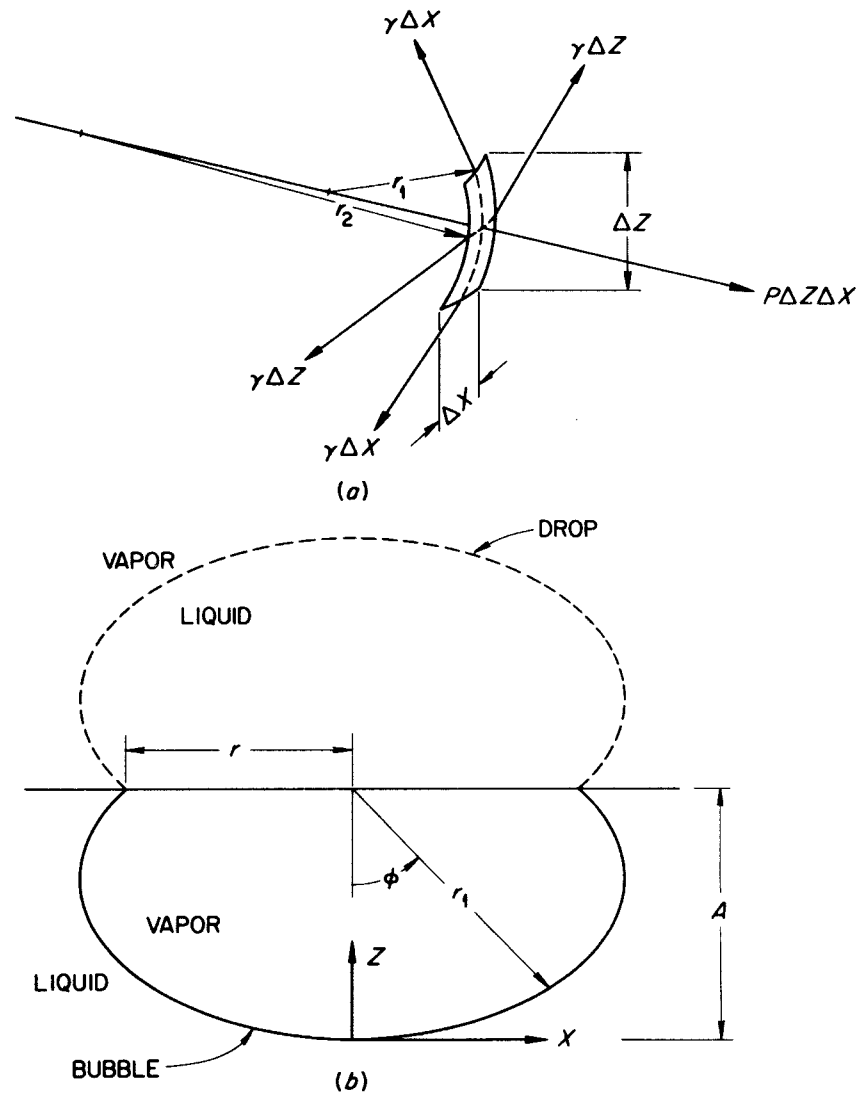


Fig. 1. Schematic View of a Sessile-Type Drop and Bubble and the Force Balance on an Infinitesimal Surface Element.

or

$$P = \gamma \left( \frac{1}{r_1} + \frac{1}{r_2} \right) . \quad (2)$$

If gravitational forces are present, the influence of the differential fluid density,  $\rho$ , must be considered. For an interface assumed to be symmetrical about an axis of revolution, the force balance equation for the bubble shown in Fig. 1-b will be

$$P - \gamma \left( \frac{1}{r_1} + \frac{1}{r_2} \right) - \frac{\rho g}{g_c} (A - z) = 0 , \quad (3)$$

where  $\rho = \rho_L - \rho_V$ . At the origin,  $r_1 = r_2 \equiv b$  and thus

$$P = \frac{2\gamma}{b} + A \frac{\rho g}{g_c} . \quad (4)$$

Furthermore, with  $r_1 = x/\sin \phi$ , Eq. (3) becomes

$$\frac{2\gamma}{b} + \frac{\rho g z}{g_c} - \gamma \left( \frac{\sin \phi}{x} + \frac{1}{r_2} \right) = 0 . \quad (5)$$

A similar derivation for the drop shown in Fig. 1-b would also result in Eq. (5). This equation can now be made dimensionless with respect to  $b$ , and after rearranging:

$$\frac{1}{R} + \frac{\sin \phi}{X} = 2 + \beta Z , \quad (6)$$

where

$$\beta \equiv \frac{g\rho b^2}{\gamma g_c} \quad (7)$$

and

$$R = \frac{r_2}{b} , \quad X = \frac{x}{b} , \quad \text{and } Z = \frac{z}{b} .$$

Equation (6) can be transposed into Cartesian coordinates by substituting



$$\frac{1}{R} \equiv \frac{d^2 Z/dX^2}{[1 + (dZ/dX)^2]^{3/2}}$$

and

$$\sin \phi \equiv \frac{dZ/dX}{[1 + (dZ/dX)^2]^{1/2}}$$

to obtain

$$\frac{d^2 Z}{dX^2} + \left[ 1 + \left( \frac{dZ}{dX} \right)^2 \right] \frac{dZ}{XdX} = (2 + \beta Z) \left[ 1 + \left( \frac{dZ}{dX} \right)^2 \right]^{3/2}, \quad (8)$$

which is a second-order nonlinear differential equation, with boundary conditions:

$$X = 0 \quad ; \quad Z = 0$$

$$X = 0 \quad ; \quad dZ/XdX = 1$$

Although Eq. (8) cannot be solved analytically in terms of ordinary functions, its numerical solution is described in the next section.

#### NUMERICAL SOLUTION OF THE INTERFACIAL EQUATION

Equation (6) can be rearranged to read

$$R = \frac{1}{2 + \beta Z - (\sin \phi)/X} \quad (9)$$

and by definition:

$$\frac{d\phi}{d\phi} \equiv 1 \quad ,$$

$$\frac{dX}{d\phi} \equiv R \cos \phi = F(X, Z, \phi) \quad , \quad (10)$$

$$\frac{dZ}{d\phi} \equiv R \sin \phi = G(X, Z, \phi) \quad . \quad (11)$$

As long as  $\beta Z > 0$ , R will always be finite.

A numerical technique of fourth-order accuracy developed by Runge-Kutta<sup>9</sup> was selected to solve the set of simultaneous Eqs. (9), (10), and (11); the iterative equations describing this technique are:

$$X_{n+1} = X_n + \frac{1}{6} (k_0 + 2k_1 + 2k_2 + k_3) + O(\Delta\phi)^5, \quad (12)$$

$$Z_{n+1} = Z_n + \frac{1}{6} (m_0 + 2m_1 + 2m_2 + m_3) + O(\Delta\phi)^5, \quad (13)$$

$$\phi_{n+1} = \phi_n + \Delta\phi,$$

where

$$k_0 = \Delta\phi F(X_n, Z_n, \Delta\phi),$$

$$k_1 = \Delta\phi F\left(X_n + \frac{1}{2}k_0, Z_n + \frac{1}{2}m_0, \phi + \frac{1}{2}\Delta\phi\right),$$

$$k_2 = \Delta\phi F\left(X_n + \frac{1}{2}k_1, Z_n + \frac{1}{2}m_1, \phi + \frac{1}{2}\Delta\phi\right),$$

$$k_3 = \Delta\phi F(X_n + k_2, Z_n + m_2, \phi + \Delta\phi),$$

$$m_0 = \Delta\phi G(X_n, Z_n, \Delta\phi),$$

$$m_1 = \Delta\phi G\left(X_n + \frac{1}{2}k_0, Z_n + \frac{1}{2}m_0, \phi + \frac{1}{2}\Delta\phi\right),$$

$$m_2 = \Delta\phi G\left(X_n + \frac{1}{2}k_1, Z_n + \frac{1}{2}m_1, \phi + \frac{1}{2}\Delta\phi\right),$$

$$m_3 = \Delta\phi G(X_n + k_2, Z_n + m_2, \phi + \Delta\phi),$$

and where the symbol  $O(\Delta\phi)^5$  represents a term which is small, of the order  $(\Delta\phi)^5$ , when  $\Delta\phi$  is small.

Equations (12) and (13) are of a form that can be readily transformed into a computer program.

## COMPUTER PROGRAM

The computer program for the solution of the interfacial equation and for the calculation of the various output parameters is listed in Appendix C. The program consisted of four parts which are discussed below.

Solution of the Differential Equation. Two subroutines in both single and double precision and consisting of four iteration loops were written to solve Eqs. (12) and (13). The subroutines RHOS and RHOD calculate the values of R and supply the values of the functions F and G to the subroutines RUNGKS and RUNGKD. These latter subroutines calculate the values of the coefficients  $k_i$  and  $m_i$  and the new values of X, Z, and  $\phi$  for reintroduction in RHOS and RHOD to continue the iterative procedure. The iteration procedure is initiated by equating X, Z, and  $\phi$  to zero and R to one.

Solution for  $h/a$  and  $V/a^3$  versus  $\beta$  and  $\phi$ . The pressure and volume within the attached bubble are calculated from X, Z, and  $\phi$ . The pressure relation is given by Eq. (4) and can be simplified by using Eq. (7) and the definition of the specific cohesion,

$$a^2 \equiv \frac{2\gamma g_c}{\rho g} , \quad (14)$$

to obtain

$$h/a = \sqrt{2/\beta} + Z_r \sqrt{\beta/2} , \quad (15)$$

where

$$Z_r = Z(x = r) = A ,$$

and

$$h = g_c P / \rho g .$$

The volume relation can be obtained from the integration of

$$d\left(\frac{V}{b^3}\right) = \pi X^2 dZ , \quad (16)$$

where X and dZ can be obtained from Eq. (6). Integrating the resulting equation by parts gives the relationship:

$$\frac{V}{b^3} = \frac{\pi X^2}{\beta} \left[ 2 + \beta Z - \frac{2 \sin \phi}{X} \right]. \quad (17)$$

Upon substituting Eqs. (6), (14), and (15) into Eq. (17), the final expression for the dimensionless volume is obtained:

$$\frac{V}{a^3} = \pi \frac{r}{a} \left[ \left( \frac{r}{a} \right) \left( \frac{h}{a} \right) - \sin \phi \right], \quad (18)$$

where

$$\frac{r}{a} = X_r \sqrt{\beta/2}$$

is the dimensionless radius of attachment.

Solution for  $h/a$  and  $V/a^3$  versus  $\beta$  and  $r/a$ . To obtain the pressure and volume within attached bubbles for a given radius of attachment from the numerical solutions  $X$ ,  $Z$ ,  $\phi$ , of the interfacial equation, several conditional "IF" statements were required. The interrelationship of  $h/a$ ,  $\beta$ ,  $r/a$ , and  $\phi$  are shown schematically in Fig. 2. The iterative solution of the interfacial equation proceeds along constant  $\beta$  lines for given steps of  $\Delta\phi$ . A conditional check is made to note the intersection of the given  $r/a$  curve (denoted by  $\square$ ), and the values at the point of crossing are determined by linear interpolation. Since  $r/a$  is multi-valued, an additional check is necessary to note when the increasing values of  $r/a$  start to decrease at  $\phi = n\pi/2$ ,  $n = 1, 5 \dots$  (denoted by  $\circ$ ), or when decreasing values start at  $\phi = n\pi/2$ ,  $n = 3, 7 \dots$ . In this manner, solutions for many values of  $r/a$  can be obtained for a given value of  $\beta$ .

Solutions for  $\bar{h}/a$  and  $\bar{V}/a^3$  versus  $r/a$ . These solutions were somewhat more difficult to obtain than those described above since it was necessary to increment  $\beta$  as well as  $\phi$ . Both of the conditional checks described above for crossing a given value of  $r/a$  and a change from increasing to decreasing  $r/a$  values were required as well as a check for the change from increasing to decreasing values of  $h/a$  (denoted by  $\Delta$  in Fig. 2).

ORNL-DWG 71-7610

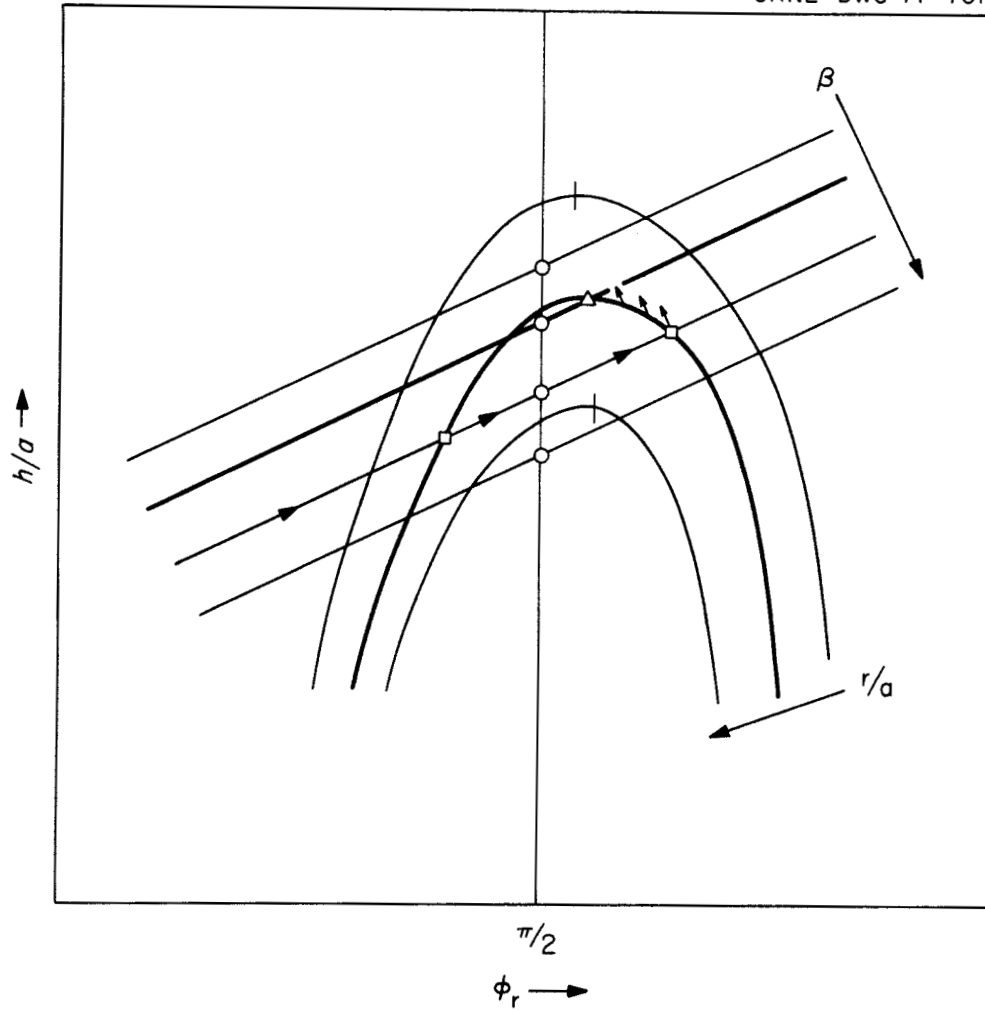


Fig. 2. Schematic Representation of the Relationships Between  $h/a$ ,  $\beta$ ,  $r/a$ , and  $\phi_r$ .

For a given value of  $\beta$ ,  $h/a$  is a multi-valued function so that the choice of increasing or decreasing  $\beta$  to approach  $\bar{h}/a$  must be carefully considered. Furthermore, the direction of approach to  $\bar{h}/a$  along the given value of  $r/a$  must also be carefully considered. To insure the most trouble-free solution over the entire  $h/a$  versus  $\phi$  field, a decremental approach from right to left (as shown by the arrows in Fig. 2) was chosen.

To reduce the number of iterations required to locate  $\bar{h}/a$ , an estimate of the value of  $\beta$  is calculated from equations fitted to a few preliminary results. The initial  $\beta$  value is then decremented along first a coarse grid, and finally along an extra fine grid to obtain the final solution using double precision.

#### Range, Running Time, and Accuracy

The ranges of the computer program as presently written are  $0 < \phi < 360^\circ$ ,  $0.1 \leq r/a \leq 2.0$ , and  $0.02 \leq \beta \leq 150$ ; however, these can be easily extended at some sacrifice of either the running time or accuracy. The average running time for the program to obtain a value of  $\bar{h}/a$  for a given value of  $r/a$  is approximately 10 seconds on the IBM 360-91 Computer system. The average running time for the other programs is considerably shorter per solution.

An estimate of the accuracy (to be given later) was obtained by comparing the values of  $h/a$  as a function of  $\phi$  for various values of  $\beta$ ,  $\Delta\phi$ , and for single and double precision.

The results of the computer solution are discussed in the next section.

### RESULTS

The results in both tabular and graphical form are presented in this section and in the Appendix.

The profile of a bubble for  $\beta = 0.8$  is shown in Fig. 3. The profile is shown extended to  $\phi = 360^\circ$ , which would be possible if a suitable

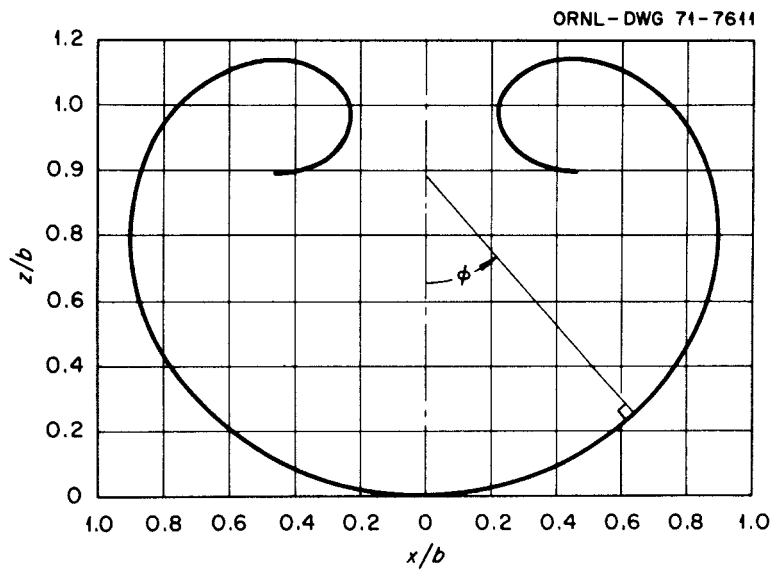


Fig. 3. Profile of a Bubble with  $\beta = 0.8$  for  $0^\circ \leq \phi \leq 360^\circ$ .

form of attachment were provided, and the center of buoyancy were to remain on the z axis.

A tabulation of  $\beta$ ,  $x/b$ ,  $z/b$ ,  $h/a$ , and  $V/a^3$  for various values of  $\phi$  are presented in Tables B.1 through B.6 (in Appendix B). Plots of  $h/a$  and  $V/a^3$  versus  $\phi$  for various  $r/a$  are shown in Figs. 4 and 5, respectively. Figure 4 clearly shows the attainment of a maximum value of  $h/a$  ( $\bar{h}/a$ ) for a given radius of attachment. (This is the basis of the maximum-bubble-pressure technique<sup>4</sup> for the measurement of surface tension.) In addition, there is a minimum value of  $h/a$  as well as a maximum value for  $V/a^3$ .

The values of  $\bar{h}/a$  and the corresponding values of  $\bar{V}/a^3$ ,  $\bar{\beta}$ ,  $\bar{\phi}$ ,  $\bar{x}/b$ ,  $\bar{z}/b$  for various values of  $r/a$  are given in Table 1, and various cross-plots of these variables are given in Figs. A.1 through A.4 (Appendix A). These plots show that both  $\bar{h}/a$  and  $\bar{\phi}_r$  approach asymptotic values of  $\sqrt{2}$  and  $180^\circ$ ,\* respectively. Thus, the maximum pressure difference ( $\bar{h}/a$ ) that a large tube can sustain will be very nearly independent of tube diameter.

A least-squares, polynomial fit of the computer solutions for various formulations of  $\bar{h}/a$  and  $r/a$  were made. The formulation that gave the best fit was

$$\frac{a}{\bar{h}} - \frac{a}{r} = f \left( \frac{a}{\bar{h}} - \frac{r}{a} \right), \quad (19)$$

which is of the same form as the perturbation solutions of Rayleigh-Schrödinger. For this reason, Eq. (19) was fitted to the data of Table 1 by the relationship:

$$F(y) = \frac{f(y) - i_0 + i_1 y + i_2 y^2}{y^3} = i_3 + i_4 y + i_5 y^2 + \dots, \quad (20)$$

where  $i_0$ ,  $i_1$ , and  $i_2$  are the coefficients of the Rayleigh-Schrödinger solution and  $i_3$ ,  $i_4$ ,  $i_5$ , ... were determined by the least-squares procedure and are listed in Table 2.

---

\* These values can be obtained by the solution of Eq. (3) with  $1/r_1 = 0$  and  $1/b = 0$ .



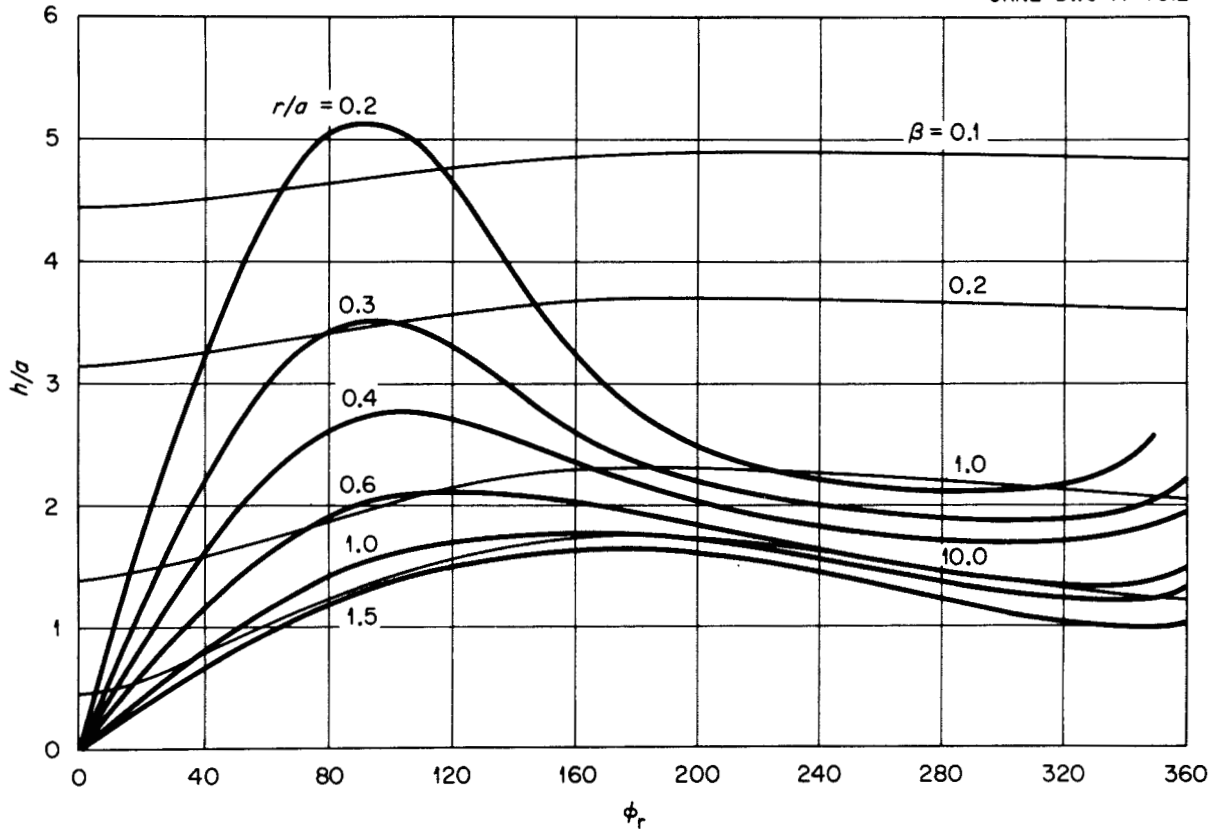


Fig. 4. Variation of the Dimensionless Pressure Difference,  $h/a$ , as a Function of  $\phi_r$  for Various Values of  $\beta$  and the Dimensionless Radius of Attachment,  $r/a$ .

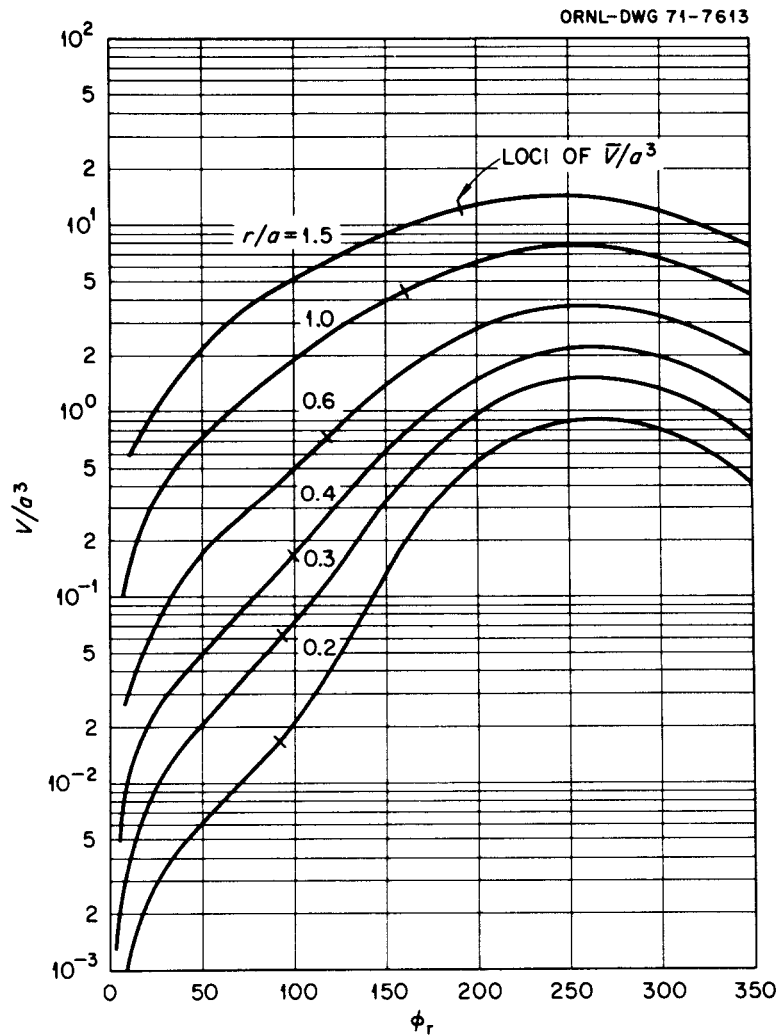


Fig. 5. Variation of the Dimensionless Volume,  $V/a^3$ , as a Function of  $\phi_r$  for Various Values of the Dimensionless Radius of Attachment,  $r/a$ .

Table 1. Maximum Values of the Pressure ( $\bar{h}/a$ ) and Corresponding Values of the Size, Shape, and Volume of Bubbles as a Function of the Radius of Attachment ( $r/a$ )

$r/a$	$\bar{\phi}$	$\bar{\beta}$	$\bar{x}/b$	$\bar{z}/b$	$\bar{h}/a$	$\bar{V}/a^3$
0.12	90.646	0.0290810	0.995156	0.999705	8.413519	0.003651
0.14	90.795	0.0397216	0.993412	0.998120	7.236465	0.005806
0.16	91.427	0.0521086	0.991243	1.00397	6.357323	0.008787
0.18	91.906	0.0662774	0.988791	1.00649	5.676507	0.012624
0.20	92.411	0.082286	0.986012	1.00865	5.134652	0.017439
0.22	92.906	0.100192	0.982929	1.00988	4.693892	0.023404
0.24	93.420	0.120066	0.979526	1.01064	4.328985	0.030656
0.26	93.945	0.141985	0.975814	1.01077	4.022445	0.039323
0.28	94.488	0.166037	0.971786	1.01039	3.761790	0.049570
0.30	95.474	0.192565	0.966824	1.01574	3.537926	0.062105
0.325	96.472	0.229022	0.960416	1.01752	3.299450	0.080293
0.350	97.476	0.269500	0.953463	1.01785	3.097815	0.101911
0.375	98.987	0.315035	0.944859	1.02327	2.925744	0.128876
0.400	100.225	0.365084	0.936222	1.02319	2.777713	0.158475
0.425	101.985	0.421688	0.925568	1.02746	2.649595	0.197373
0.450	103.483	0.483756	0.914990	1.02640	2.538105	0.239818
0.475	104.821	0.551689	0.904402	1.02173	2.440625	0.286173
0.50	107.164	0.631617	0.889730	1.02464	2.355273	0.346254
0.55	111.986	0.822982	0.857398	1.02159	2.214232	0.501889
0.60	117.488	1.072133	0.819487	1.00938	2.104842	0.708170
0.65	123.990	1.407182	0.774913	0.986809	2.019914	0.987762
0.70	130.993	1.853431	0.727151	0.950582	1.953875	1.347727
0.75	137.489	2.414075	0.682654	0.902832	1.902104	1.768822
0.80	140.664	2.977900	0.655617	0.853059	1.860445	2.136163
0.90	152.491	4.841565	0.578448	0.742939	1.798649	3.270626
1.00	158.492	7.100181	0.530738	0.648972	1.753511	4.356567
1.10	162.989	10.070060	0.490221	0.567348	1.718720	5.521721
1.20	165.994	13.866110	0.455742	0.497922	1.690847	6.736407
1.30	167.994	18.715220	0.424972	0.438376	1.667904	8.005399
1.40	169.991	25.16100	0.394711	0.385323	1.648640	9.386485
1.50	171.489	33.48783	0.366575	0.339160	1.632205	10.839000
1.60	172.494	44.16429	0.340486	0.299033	1.618007	12.356187
1.70	173.488	58.14618	0.315285	0.263383	1.605608	13.971941
1.80	173.998	75.94175	0.292110	0.232455	1.594682	15.640580
1.90	174.987	99.7358	0.268978	0.204340	1.584975	17.453834
2.00	175.489	130.1581	0.247919	0.180031	1.576295	19.314144

Table 2. Coefficients for the Polynomial Equations  
Fitted to the Computer Solution

Coefficients	Eq. (19)	Eq. (21)
$i_0$	1.00000	-0.00090
$i_1$	-0.66667	1.04439
$i_2$	-0.66667	-0.47175
$i_3$	0.03230	1.43283
$i_4$	-5.52833	-4.59801
$i_5$	61.19134	5.38228
$i_6$	-351.38141	-2.73720
$i_7$	1099.76625	0.51837
$i_8$	-1930.93994	
$i_9$	1913.36384	
$i_{10}$	-1003.22519	
$i_{11}$	216.93848	

The main disadvantage of Eq. (19) is that an iterative procedure is necessary to calculate  $a/\bar{h}$ . A simpler formulation, but less accurate, was also fitted to the computer results:

$$\frac{a}{\bar{h}} = f\left(\frac{r}{a}\right). \quad (21)$$

The coefficients for the polynomial fit of Eq. (21) are also listed in Table 2.

The accuracy of these two polynomial fits is discussed in the next section.

#### DISCUSSION OF RESULTS

An estimate of the accuracy of the computer results and comparisons with previous results are presented in this section.

Estimation of the Accuracy. Results were obtained for  $h/a$  versus  $\phi$  for  $\beta = 0.1$  and  $100.0$  with three values of  $\Delta\phi = 1^\circ$ ,  $1/2^\circ$ , and  $1/4^\circ$  using both single and double precision. There was no change in  $h/a$  (to the seventh decimal place) as  $\Delta\phi$  was decreased from  $1^\circ$  to  $1/4^\circ$  when double precision was used for  $\beta = 0.1$  and only  $0.00008\%$  change for  $\beta = 100.0$ . The single precision results are plotted in Fig. 6, where the percent difference is with reference to the double precision,  $\Delta\phi = 1/4^\circ$ , values. As can be seen, an interval less than  $\Delta\phi = 1^\circ$  decreased the accuracy of the results because of rounding errors when single precision was used.

Except for the maximum pressure results listed in Table 1, all the tabulated results were computed using single precision and interval  $\Delta\phi = 1^\circ$ . The values listed in Table 1 were calculated using double precision and are good to at least the seventh decimal place. The other tabulated results are good to at least the fifth decimal place.

Comparison with Previous Results. As anticipated, the careful, tedious hand calculations of Bashforth and Adams (which required a number of years to complete) were in good agreement (to the fifth decimal place) with the present computer solution. Trouble, however, develops when the Bashforth and Adams tables are singly and doubly interpolated to apply

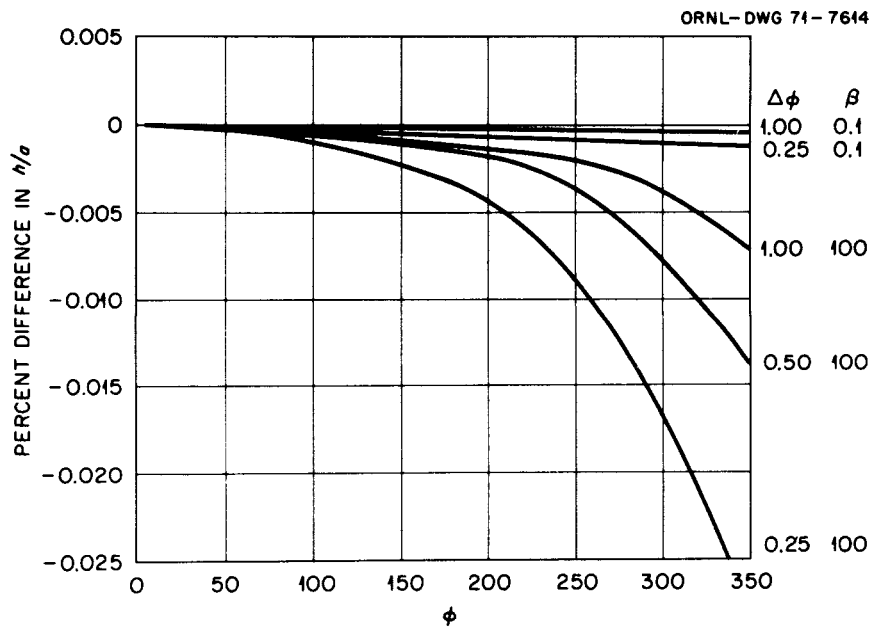


Fig. 6. Comparison of the Single Precision Results for  $h/a$  with the Double Precision,  $\Delta\phi = 1/4$ , Values as a Function of  $\phi$ ,  $\Delta\phi$ , and  $\beta$ .

their results to practical calculations. Sudgen,<sup>10</sup> "by careful interpolation" of Bashforth's tables, constructed a table for calculating surface tension by the maximum-bubble-pressure method. (This table is the one most often referred to in current literature on surface tension.) The percent difference between our solution and Sudgen's as a function of  $r/a$  is shown in Fig. 7. The maximum difference is -0.1%.

Although an error of 0.1% can be neglected for some studies at elevated temperatures (where other errors are more significant), this magnitude of error can be significant for many measurements made at room temperature, where theoretical studies of small changes in the molecular structure of the interface are being conducted. Furthermore, this error can be magnified by as much as 20 times when the two tube, differential technique is used to measure surface tension.

To be particularly noted in Fig. 7 is that the Rayleigh-Schrödinger solution is in better agreement with the computer solution than Sudgen's results all the way from  $0 \leq r/a \leq 0.45$ . This range of  $r/a$  covers a large portion of the surface tension studies that have been conducted in the past. In fact, the Rayleigh-Schrödinger equation is in error by less than 1.05% all the way to  $r/a = 1.0$ . Thus, this much simpler analytic solution can be used in many cases where precise surface tension values are not needed.

Also shown in Fig. 7 are the deviations of Eqs. (19) and (21) from the computer solutions. Equation (19) agrees to within  $\pm 0.05\%$  all the way to  $r/a = 1.5$ . The simpler Eq. (21) agrees to within  $\pm 0.07\%$  from  $0.2 \leq r/a \leq 1.5$ ; but Schrödinger's equation is recommended for  $r/a < 0.2$ . The main disadvantages of Eqs. (19) and (21) is that double precision should be used in their solution, especially at the larger values of  $r/a$ .

Baumeister and Hamill presented their results as plots of droplet volumes and heights as functions of droplet radii and contact angles. In this form, their results could not be conveniently compared with the present results. In addition, their results were given to only the third significant figure.

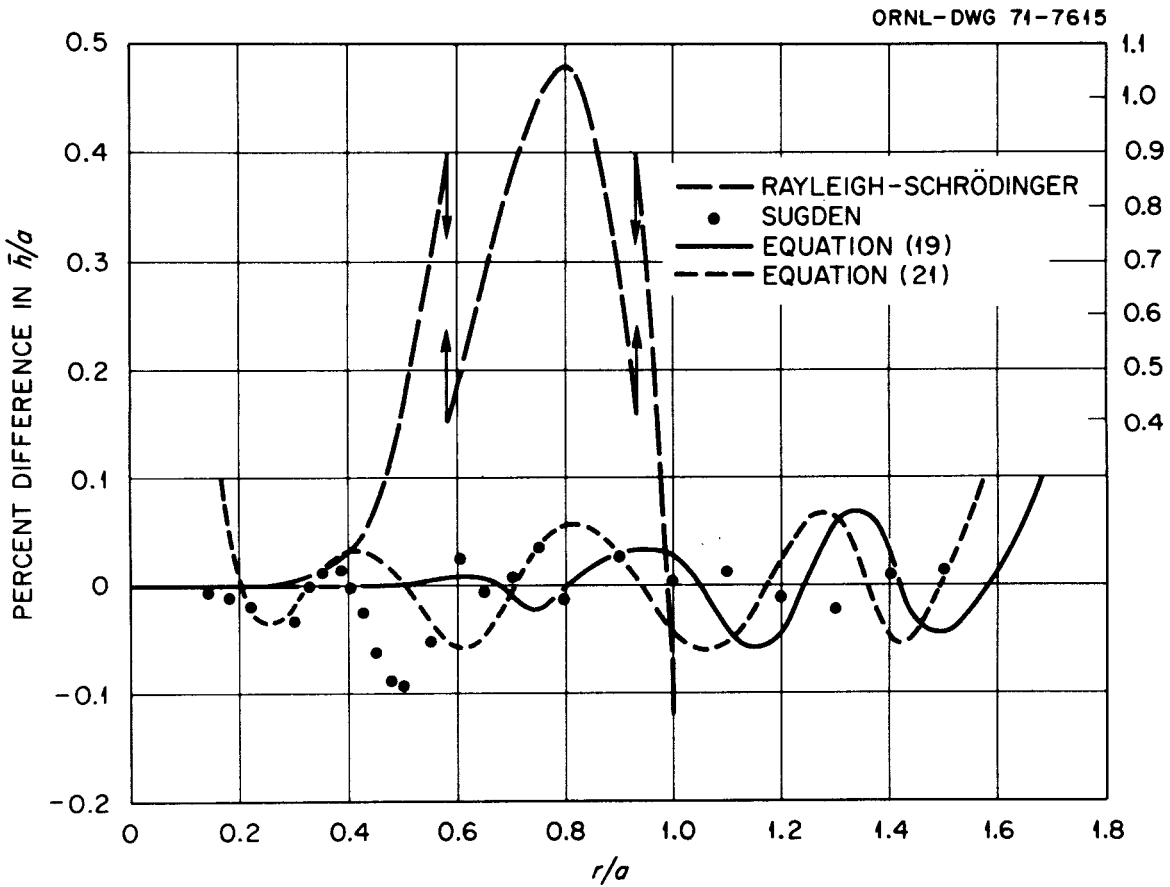


Fig. 7. Deviations of Previous Solutions and Present Polynomial Equations from the Present Computer Solution of the Maximum-Bubble Pressure.



## CONCLUSIONS

A computer program was written to solve the second-order, nonlinear, differential equation describing the axially symmetric interface between two immiscible fluids. The present solution is limited to sessile-shaped drops and bubbles; the solution for pendant-shaped drops and bubbles requires a different approach and will be given in a later report. All of the present results are accurate to at least the fifth decimal place with some results accurate to the seventh decimal place.

The results are presented in a form that is useful in the analysis of boiling and condensing heat transfer, superheat, critical constants, and in the measurements of contact angles and surface tension. In addition, these results may be of use in the design of equi-stressed shells for containment vessels (i.e., above-ground water tanks, under-water storage of liquids and gases, lighter-than-air ballons, and submerged marine laboratories). The computer program is listed so that a wider range and number of variables can be obtained as desired.

## REFERENCES

1. F. Kreith, Principles of Heat Transfer, pp. 308-437, International Textbook Company, Scranton, Pennsylvania, 1st ed., 1959.
2. J. A. Edwards and H. W. Hoffman, Superheat Correlation for Boiling Alkali Metals, Proceedings of the Fourth International Heat Transfer Conference, Versailles, September 1970 (under the book title "Heat Transfer 1970"), Elsevier Publishing Company, Amsterdam, Netherlands, 1970.
3. A. V. Grosse, The Relationship Between the Surface Tension and Energies of Liquid Metals and Their Critical Temperatures, J. Inorg. Nucl. Chem., 24:147-156 (1962).
4. D. W. G. White, Theory and Experiment in Methods for the Precision Measurement of Surface Tension, Trans. ASME, 55: 757 (1962).
5. Lord Rayleigh, On the Theory of the Capillary Tube, Proc. Roy. Soc., 92 (Series A): 184-195 (1915).
6. Erwin Schrödinger, Notizüber den Kapillardruck in Gasblasen, Ann. Physik., 46: 413-418 (1915)

7. F. Bashforth and J. C. Adams, An Attempt to Test the Theories of Capillary Action by Comparing the Theoretical and Measured Forms of Drops of Fluids, University Press, Cambridge, Massachusetts, 1883.
8. K. J. Baumeister and T. D. Hamill, Liquid Drops: Numerical and Asymptotic Solutions of their Shapes, NASA-TN-D-4779, National Advisory Committee for Aeronautics, September 1968.
9. F. B. Hildebrand, Introduction to Numerical Analysis, pp. 236-239, McGraw-Hill, New York, 1956.
10. S. Sugden, The Determination of Surface Tension from Maximum Pressure in Bubbles, J. Chem. Soc., 1: 858-866 (1922).

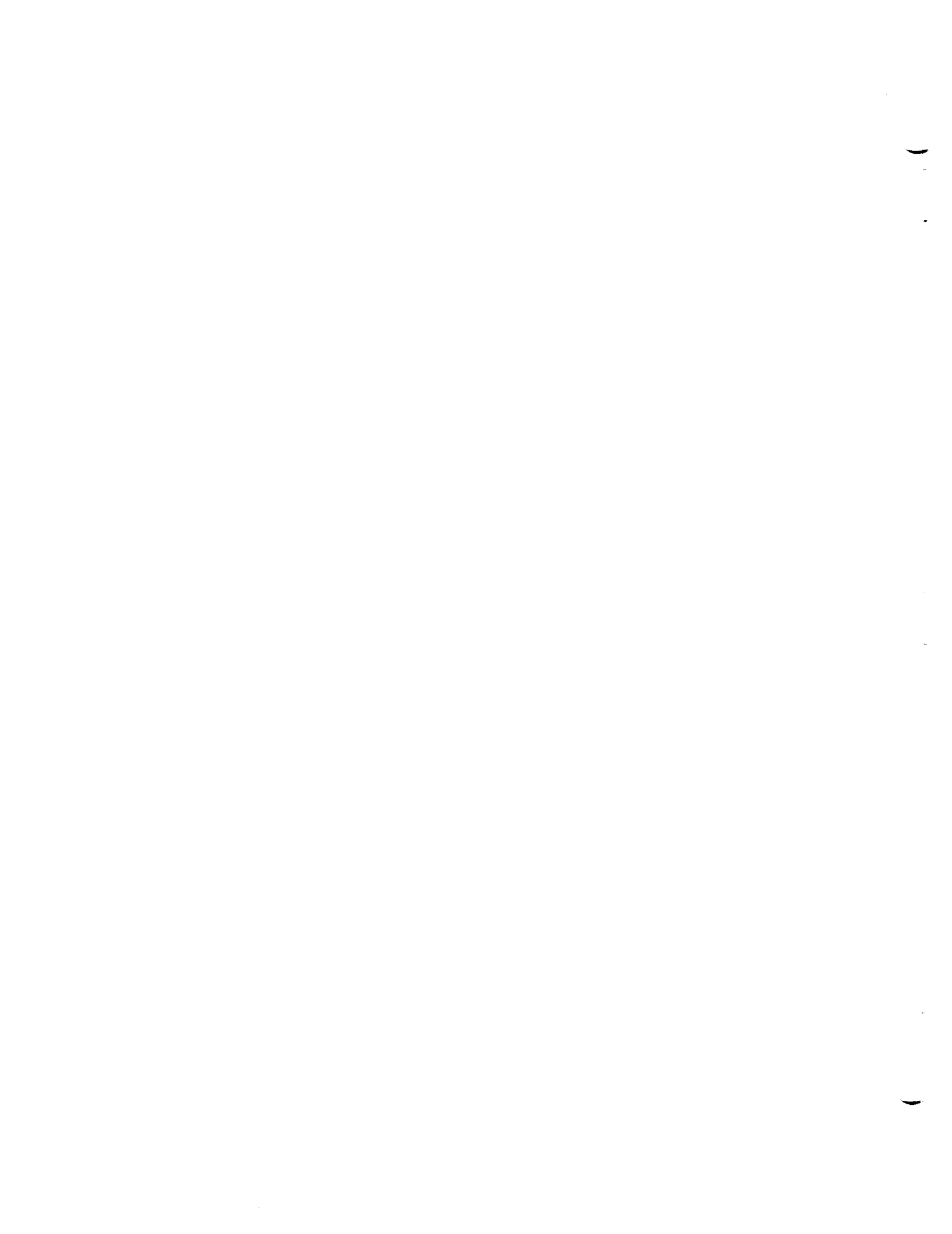
#### NOMENCLATURE

A	distance from the origin to the plane of attachment, cm
$a^2$	specific cohesion $\equiv 2\gamma g_c / \rho g$ , $\text{cm}^2$
b	radius of curvature at the vertex of the bubble, cm
g	local acceleration due to gravity, $\text{cm}/\text{sec}^2$
$g_c$	dimensional constant, $\text{dyne}\cdot\text{sec}^2/\text{g}\cdot\text{cm}$
h	pressure differential across interface, cm of fluid with density $\rho$
$\bar{h}$	maximum value of h for given value of $r/a$ , cm of fluid with density $\rho$
i	coefficients of polynomial equations
k	coefficients of numerical equations
m	coefficients of numerical equations
P	pressure differential across interface, $\text{dyne}/\text{cm}^2$
r	radius of circle of attachment, cm
$r/a$	dimensionless radius of attachment
$r_1, r_2$	principal radii of curvature of the interface, cm
R	dimensionless value of $r_2, r_2/b$
V	volume enclosed by the interface, $\text{cm}^3$

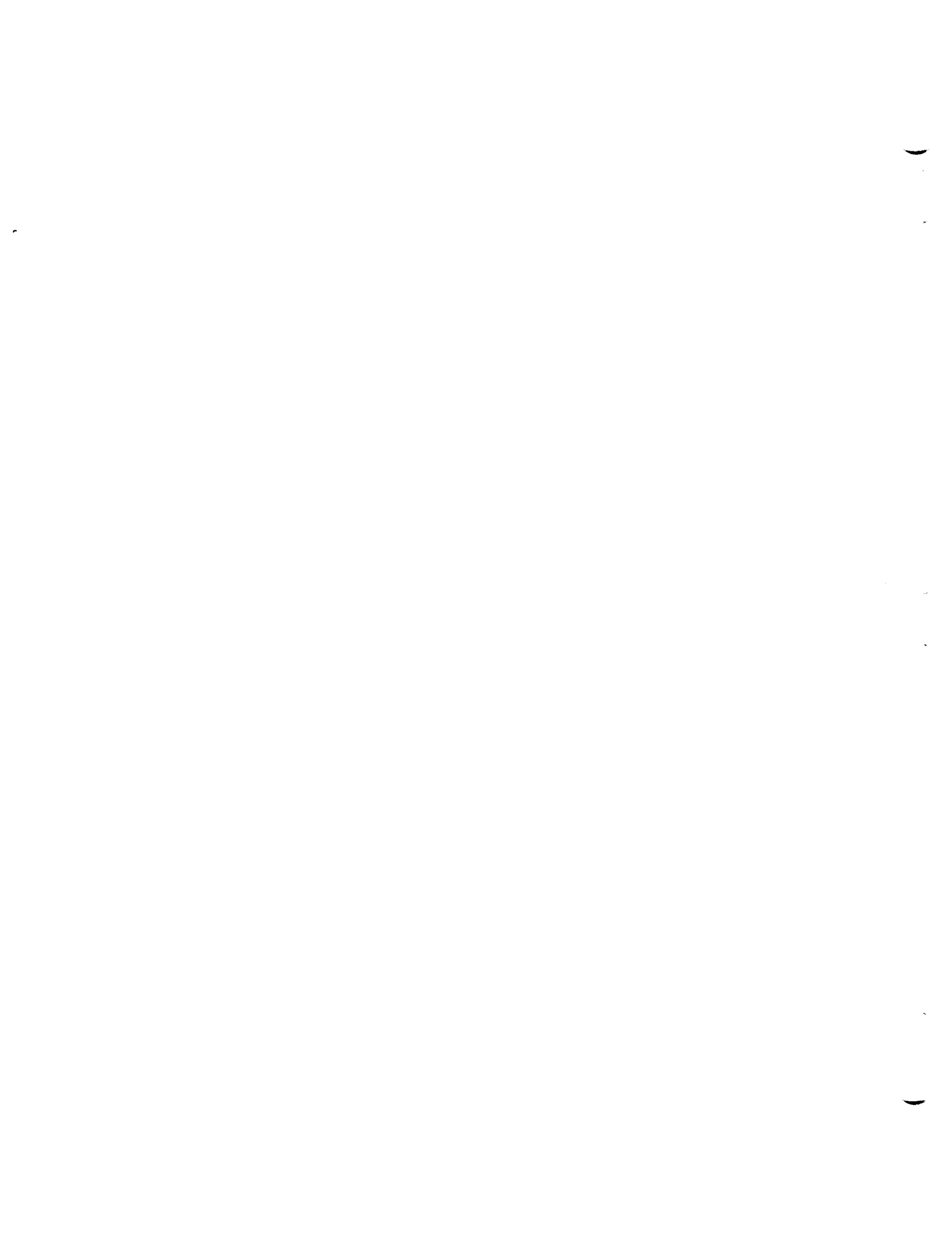
$\bar{V}$	volume enclosed by the interface for a given value of $r/a$ at $h/a = \bar{h}/a$ , $\text{cm}^3$
$x$	horizontal coordinate, $\text{cm}$
$\bar{x}$	value of $x$ for a given value of $r/a$ at $h/a = \bar{h}/a$ , $\text{cm}$
$X$	dimensionless $x$ , $x/b$
$X_r$	value of $X$ at $x = r$
$y$	independent variable in polynomial equation
$z$	vertical coordinate, $\text{cm}$
$\bar{z}$	value of $z$ for a given value of $r/a$ at $h/a = \bar{h}/a$ , $\text{cm}$
$Z$	dimensionless $z$ , $z/b$
$Z_r$	value of $Z$ at $x = r$

#### Greek Letters

$\beta$	dimensionless parameter $\equiv g\rho b^3/g_c\gamma = 2(b/a)^2$
$\bar{\beta}$	value of $\beta$ for a given $r/a$ at $h/a = \bar{h}/a$
$\gamma$	interfacial tension, $\text{dyne/cm}$
$\phi$	angle between axis of revolution and the normal to the surface
$\phi_r$	value of $\phi$ at the radius of attachment
$\bar{\phi}_r$	value of $\phi_r$ for a given $r/a$ at $h/a = \bar{h}/a$
$\rho$	positive density difference between the two fluids, $\text{g/cm}^3$



APPENDICES



#### A. PARAMETRIC CROSSPLOTS

Various crossplots of the parameters shown in Figs. 4 and 5 are given in Figs. A.1, A.2, and A.3. The maximum bubble radius as a function of the angle  $\phi_r$  for various radii of attachment is shown plotted in Fig. A.4. For  $\phi_r < 90^\circ$ , the maximum bubble radius would be the radius of attachment. Also shown in Fig. A.4 is the loci of the maximum bubble radius where the maximum bubble pressure is reached.

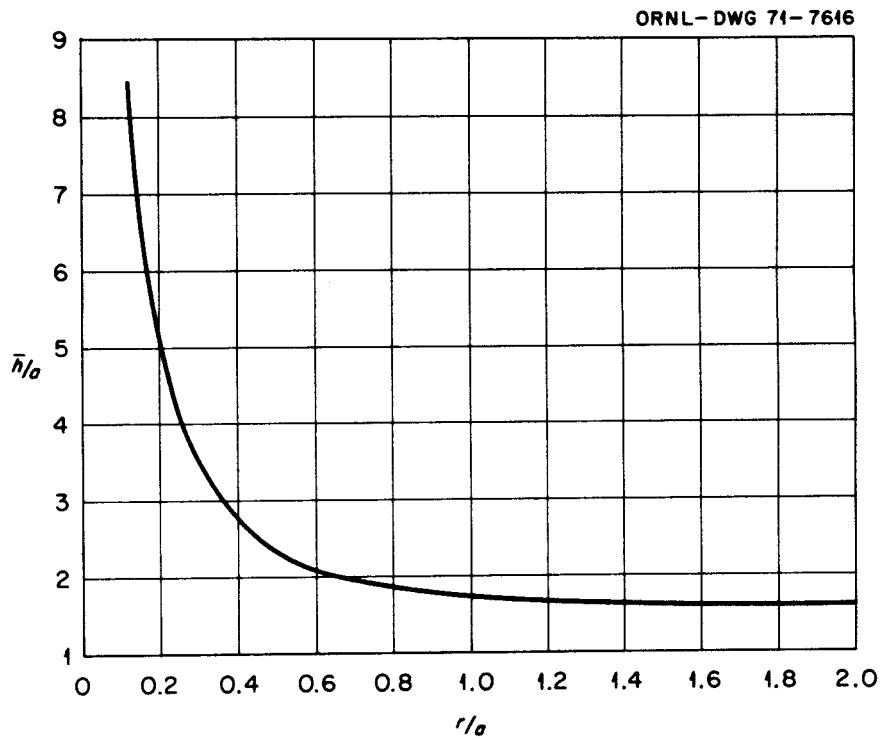


Fig. A.1. Dimensionless Maximum-Pressure-Difference Across the Interface Separating Two Fluids as a Function of the Dimensionless Radius of Attachment.



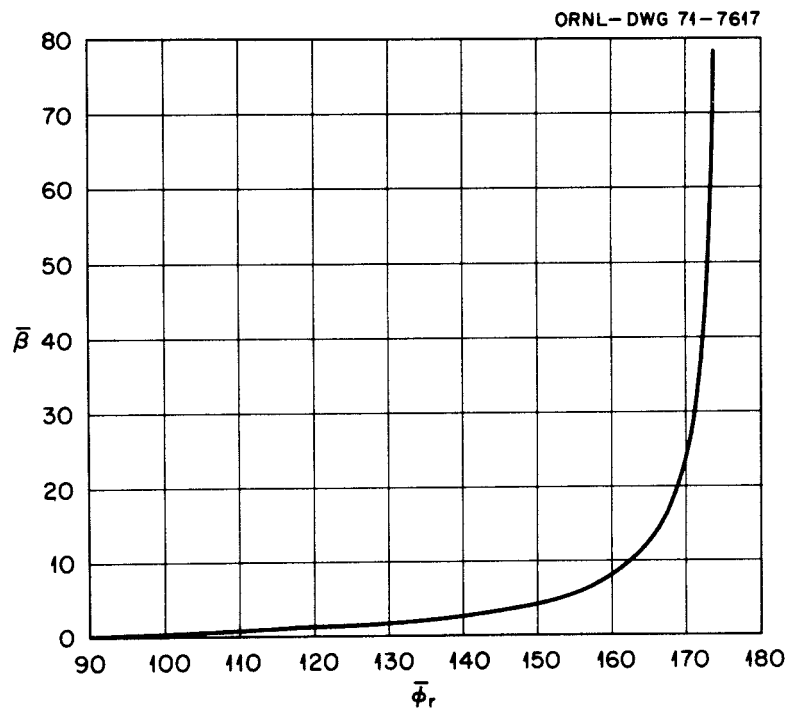


Fig. A.2. The Value of the Parameter  $\beta$  at  $h/a = \bar{h}/a$  as a Function of  $\phi_r$ .

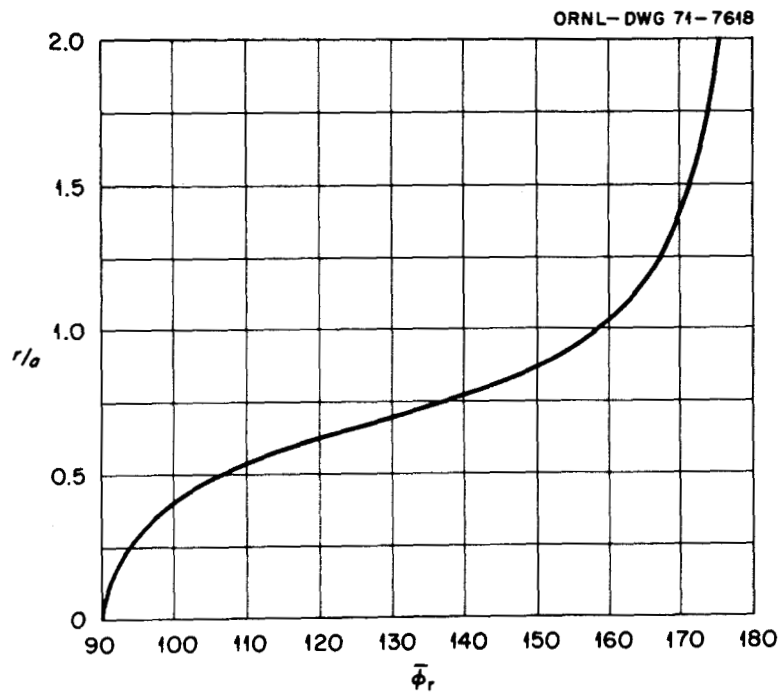


Fig. A.3. The Dimensionless Radius of Attachment as a Function of  $\bar{\phi}_r$  at  $h/a = \bar{h}/a$ .

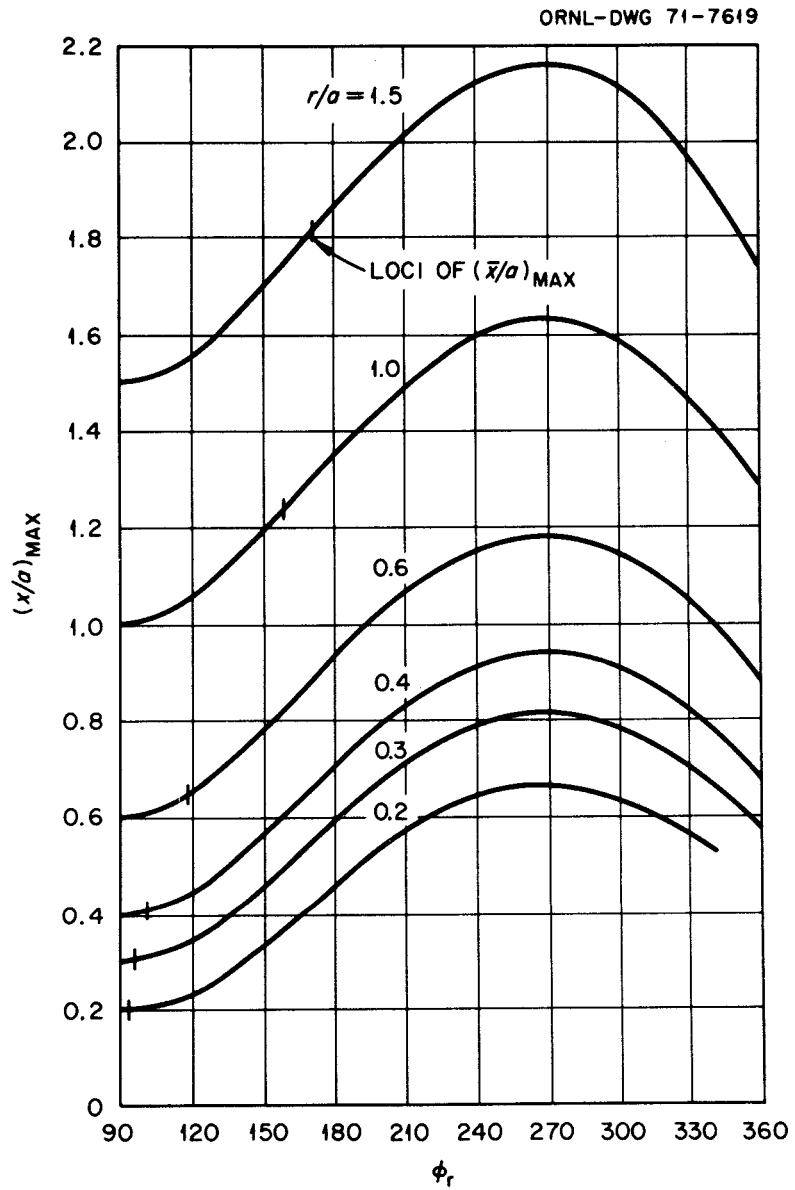
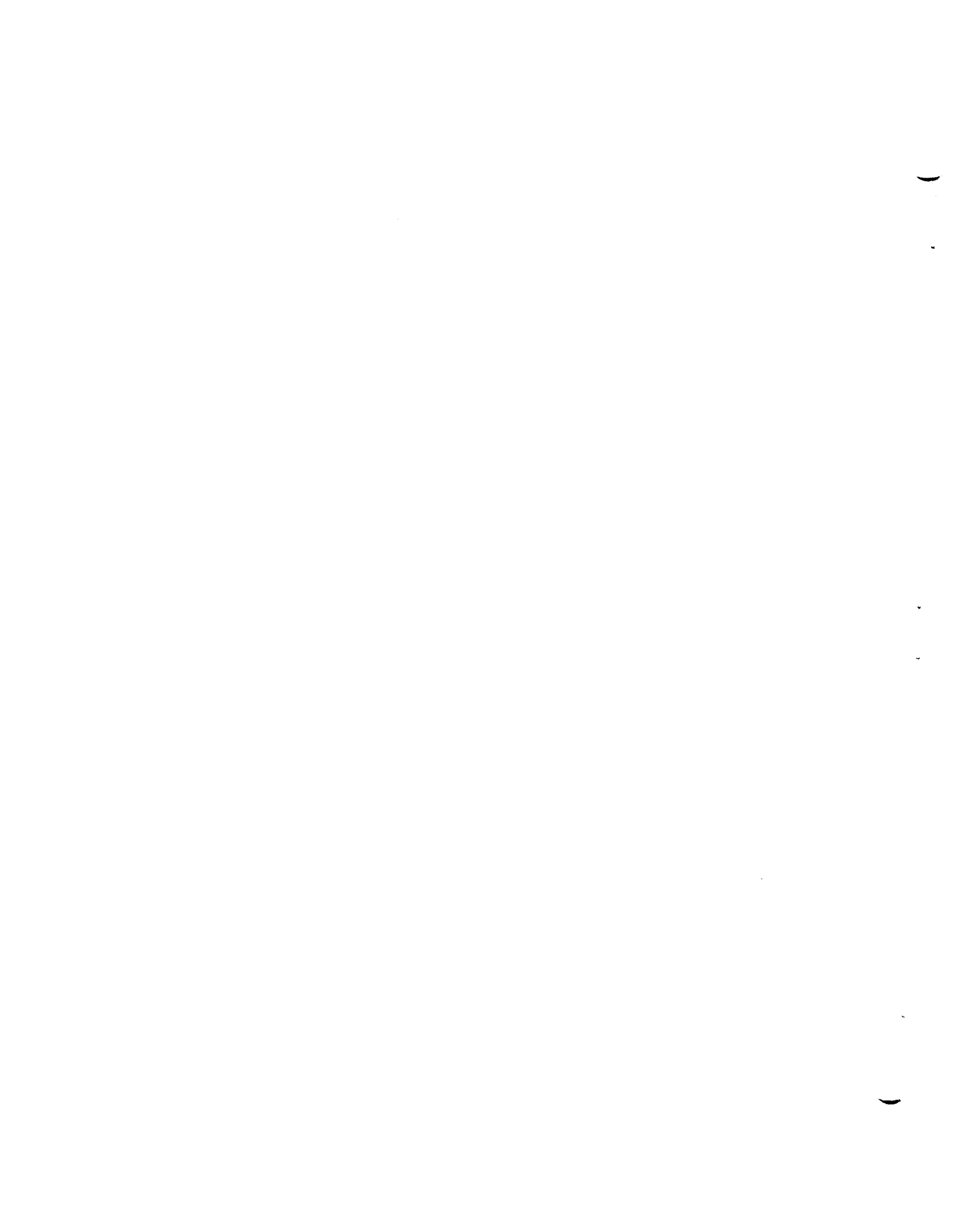


Fig. A.4. Maximum Radius of a Bubble ( $x/a$  at  $\phi = 90^\circ$ ) as a Function of  $\phi_r$  for Various Radii of Attachment ( $r/a$ ). For  $\phi_r < 90^\circ$ ,  $(x/a)_{\text{MAX}} = r/a$ .



## B. TABULATED RESULTS

The computer results for the size, shape, pressure, and volume of attached bubbles and drops for given radii of attachment are listed in Table B.1 through B.6. The Results are arranged in ascending values of  $\phi_r$ .

Table B.1. Size, Shape, Pressure, and Volume of Bubbles and Drops with a Given Radius of Attachment

$$r/a = 0.2$$

$\beta$	$\phi_r$	$x/b$	$z/b$	$h/a$	$v/a^3$
30.00	2.99	0.05168	0.00135	0.26341	0.00030
18.00	3.86	0.06667	0.00225	0.34009	0.00042
8.00	5.80	0.10000	0.00505	0.51009	0.00063
5.50	7.00	0.12061	0.00734	0.61519	0.00077
4.00	8.21	0.14142	0.01013	0.72143	0.00090
3.50	8.78	0.15119	0.01158	0.77125	0.00096
2.90	9.66	0.16609	0.01400	0.84731	0.00106
2.30	10.86	0.18650	0.01765	0.95144	0.00119
2.00	11.66	0.20000	0.02317	1.02032	0.00128
1.80	12.30	0.21082	0.02262	1.07556	0.00135
1.50	13.49	0.23094	0.02717	1.17823	0.00149
1.10	15.81	0.26968	0.03727	1.37604	0.00175
0.95	17.05	0.29019	0.04327	1.48078	0.00189
0.80	18.63	0.31623	0.05161	1.61378	0.00207
0.66	20.59	0.34816	0.06295	1.77694	0.00229
0.58	22.04	0.37139	0.07194	1.89569	0.00247
0.50	23.84	0.40000	0.08399	2.04200	0.00268
0.46	24.92	0.41703	0.09166	2.12910	0.00281
0.42	26.17	0.43644	0.10089	2.22841	0.00296
0.38	27.62	0.45883	0.11220	2.34306	0.00313
0.34	29.35	0.48507	0.12636	2.47745	0.00334
0.30	31.46	0.51640	0.14463	2.63801	0.00361
0.25	34.87	0.56569	0.17662	2.89087	0.00405
0.23	36.59	0.58977	0.19386	3.01458	0.00427
0.21	38.60	0.61721	0.21486	3.15569	0.00455
0.19	40.99	0.64889	0.24102	3.31872	0.00489
0.17	43.91	0.68599	0.27474	3.51007	0.00531
0.15	47.60	0.73030	0.31993	3.73910	0.00585
0.14	49.86	0.75593	0.34889	3.87195	0.00622
0.13	52.51	0.78446	0.38410	4.02025	0.00664
0.12	55.69	0.81650	0.42796	4.18731	0.00719
0.11	59.65	0.85280	0.48479	4.37771	0.00792
0.10	64.87	0.89443	0.56306	4.59804	0.00898
0.09	72.70	0.94281	0.68614	4.85960	0.01079
0.0828	84.85	0.98295	0.88466	5.09473	0.01444

Table B.1 (Continued)

$\beta$	$\phi$	$x/b$	$z/b$	$h/a$	$v/a^3$
0.0828	95.17	0.98295	1.05331	5.12905	0.01878
0.09	107.58	0.94281	1.24471	4.97809	0.02660
0.10	115.80	0.89443	1.35781	4.77575	0.03445
0.11	121.43	0.85280	1.42604	4.59845	0.04173
0.12	125.82	0.81650	1.47280	4.44324	0.04890
0.13	129.46	0.78446	1.50654	4.30642	0.05606
0.14	132.59	0.75593	1.53162	4.18487	0.06328
0.15	135.34	0.73030	1.55053	4.07611	0.07058
0.17	140.07	0.68599	1.57565	3.88935	0.08542
0.19	144.07	0.64889	1.58951	3.73435	0.10060
0.21	147.60	0.61721	1.59609	3.60326	0.11610
0.23	150.78	0.58977	1.59777	3.49067	0.13189
0.25	153.70	0.56569	1.59596	3.39269	0.14794
0.34	164.94	0.48507	1.56461	3.07046	0.22259
0.38	169.34	0.45883	1.54451	2.96739	0.25668
0.42	173.53	0.43644	1.52274	2.87998	0.29109
0.46	177.57	0.41703	1.50000	2.80452	0.32574
0.58	189.15	0.37139	1.42956	2.62679	0.43005
0.66	196.74	0.34816	1.38256	2.53500	0.49949
0.70	200.55	0.33806	1.35938	2.49453	0.53405
0.80	210.35	0.31623	1.30143	2.40423	0.61955
0.90	220.90	0.29814	1.24333	2.32476	0.70350
1.00	233.12	0.28284	1.18282	2.25059	0.78543
1.10	250.16	0.26968	1.11197	2.17306	0.86409
1.10	289.74	0.26968	1.01358	2.10009	0.85531
1.00	306.55	0.28284	1.00345	2.12376	0.77164
0.90	318.54	0.29814	1.01038	2.16850	0.68854
0.80	328.88	0.31623	1.02769	2.23111	0.60513

Table B.2. Size, Shape, Pressure, and Volume of Bubbles and Drops with Given Radius of Attachment

$$r/a = 0.3$$

$\beta$	$\phi_r$	$x/b$	$z/b$	$h/a$	$V/a^3$
30.0	4.55	0.07746	0.00307	0.27011	0.00165
18.0	5.87	0.10000	0.00509	0.34859	0.00215
12.0	7.20	0.12247	0.00764	0.42700	0.00264
8.0	8.83	0.15000	0.01145	0.52291	0.00325
5.5	10.66	0.18091	0.01672	0.63076	0.00393
4.0	12.53	0.21213	0.02303	0.73967	0.00464
3.5	13.41	0.22678	0.02640	0.79085	0.00496
2.9	14.77	0.24914	0.03194	0.86891	0.00547
2.3	16.63	0.27975	0.04045	0.97588	0.00618
2.0	17.87	0.30000	0.04663	1.04663	0.00667
1.8	18.88	0.31623	0.05197	1.10340	0.00745
1.7	19.45	0.32540	0.05512	1.13547	0.00727
1.5	20.76	0.34641	0.06271	1.20901	0.00779
1.25	22.85	0.37947	0.07579	1.32483	0.00861
1.2	23.35	0.38730	0.07908	1.35225	0.00881
1.1	24.46	0.40452	0.08662	1.41264	0.00925
1.0	25.74	0.42426	0.09574	1.48191	0.00977
0.95	26.46	0.43529	0.10110	1.52063	0.01005
0.9	27.24	0.44721	0.10704	1.56252	0.01038
0.8	29.05	0.47434	0.12135	1.65789	0.01113
0.7	31.28	0.50709	0.14017	1.77323	0.01206
0.66	32.32	0.52223	0.14943	1.82662	0.01250
0.58	34.79	0.55709	0.17222	1.94970	0.01358
0.5	37.92	0.60000	0.20334	2.10167	0.01499
0.46	39.86	0.62554	0.22365	2.19240	0.01588
0.42	42.13	0.65465	0.24857	2.29609	0.01695
0.38	44.87	0.68825	0.27994	2.41618	0.01829
0.34	48.25	0.72761	0.32082	2.55764	0.02000
0.3	52.62	0.77460	0.37669	2.72788	0.02236
0.25	60.61	0.84853	0.48659	3.00046	0.02715
0.23	65.36	0.88465	0.55577	3.13731	0.03036
0.21	72.20	0.92582	0.65884	3.29956	0.03559
0.195	81.53	0.96077	0.80327	3.45338	0.04423



Table B.2 (Continued)

$\beta$	$\phi$	$x/b$	$z/b$	$h/a$	$V/a^3$
0.1925	95.40	0.96694	1.01465	3.53793	0.06203
0.21	108.40	0.92582	1.19288	3.47260	0.08758
0.23	115.90	0.88465	1.27945	3.38272	0.10864
0.25	121.34	0.84853	1.33222	3.29944	0.12796
0.3	131.17	0.77460	1.40212	3.12503	0.17414
0.34	137.09	0.7276	1.42704	3.01374	0.21045
0.38	142.08	0.68825	1.43800	2.92095	0.24666
0.42	146.46	0.65465	1.44035	2.84223	0.28285
0.46	150.41	0.62554	1.43727	2.77443	0.31905
0.50	154.05	0.60000	1.43052	2.71526	0.35524
0.58	160.65	0.55709	1.41014	2.61634	0.42743
0.66	166.63	0.52223	1.38465	2.53620	0.49919
0.7	169.45	0.50709	1.37088	2.50133	0.53471
0.8	176.18	0.47434	1.33487	2.42538	0.62303
0.9	182.56	0.44721	1.29805	2.36147	0.70984
1.0	188.74	0.42426	1.26124	2.30604	0.79517
1.1	194.79	0.40452	1.22489	2.25680	0.87863
1.2	200.82	0.38730	1.18910	2.21206	0.96038
1.5	219.70	0.34641	1.08403	2.09350	1.19399
1.7	234.58	0.32540	1.01218	2.01784	1.33856
1.7	304.88	0.32540	0.83893	1.85810	1.29849
1.2	337.48	0.38730	0.87818	1.97123	0.91837
1.1	343.30	0.40452	0.89730	2.01386	0.84032
1.0	349.15	0.42426	0.92136	2.06571	0.76142
0.9	355.15	0.44721	0.95155	2.12903	0.68168

Table B.3. Size, Shape, Pressure, and Volume of Bubbles and Drops with Given Radius of Attachment

$$r/a = 0.4$$

$\beta$	$\phi_r$	$x/b$	$z/b$	$h/a$	$V/a^3$
30.0	6.17	0.10328	0.00548	0.27941	0.00533
18.0	7.98	0.13333	0.00912	0.36068	0.00692
12.0	9.79	0.16330	0.01372	0.44187	0.00850
8.0	12.02	0.20000	0.02063	0.54126	0.01047
5.5	14.54	0.24121	0.03019	0.65309	0.01270
4.0	17.13	0.28284	0.04173	0.76612	0.01504
3.5	18.35	0.30237	0.04787	0.81926	0.01613
2.9	20.24	0.33218	0.05808	0.90040	0.01786
2.3	22.86	0.37300	0.07385	1.01170	0.02030
2.0	24.63	0.40000	0.08546	1.08546	0.02196
1.8	26.06	0.42164	0.09548	1.14468	0.02332
1.5	28.78	0.46188	0.11589	1.25507	0.02594
1.25	31.84	0.50596	0.14108	1.37644	0.02897
1.1	34.23	0.53936	0.16228	1.46875	0.03139
1.0	36.17	0.56569	0.18038	1.54176	0.03341
0.8	41.32	0.63246	0.23257	1.72823	0.03897
0.66	46.69	0.69631	0.29255	1.90883	0.04512
0.58	50.97	0.74278	0.34404	2.04222	0.05041
0.5	56.89	0.80000	0.41997	2.20998	0.05828
0.46	60.93	0.83406	0.47434	2.31263	0.06413
0.42	66.32	0.87287	0.54940	2.43395	0.07262
0.38	74.69	0.91766	0.66956	2.58601	0.08785
0.36	97.25	0.94281	0.98565	2.77520	0.14837
0.38	105.99	0.91766	1.09093	2.76968	0.18416
0.42	115.44	0.87287	1.18463	2.72505	0.23502
0.46	121.96	0.83406	1.23412	2.67701	0.27950
0.5	127.16	0.80000	1.26371	2.63185	0.32143
0.58	135.45	0.74278	1.12924	2.55291	0.40169
0.66	142.15	0.69631	1.29953	2.48730	0.47925
0.7	145.12	0.67612	1.29854	2.45854	0.51723
0.8	151.82	0.63246	1.28804	2.39577	0.61073
0.9	157.75	0.59628	1.27074	2.34315	0.70194
1.0	163.17	0.56569	1.24977	2.29794	0.79124
1.1	168.21	0.53936	1.22692	2.25831	0.87839

Table B.3 (Continued)

$\beta$	$\phi$	$x/b$	$z/b$	$h/a$	$V/a^3$
1.2	172.98	0.51640	1.20312	2.22293	0.96372
1.25	175.29	0.50596	1.19105	2.20652	1.00587
1.5	186.20	0.46188	1.13075	2.13396	1.20846
1.7	194.51	0.43386	1.08367	2.08375	1.36230
2.0	206.81	0.40000	1.01557	2.01557	1.57998
2.5	229.01	0.35777	0.90542	1.90671	1.90695
2.5	310.00	0.35777	0.71442	1.69317	1.81377
2.0	331.06	0.40000	0.73401	1.73401	1.47971
1.7	342.67	0.43386	0.76316	1.78825	1.27326
1.5	350.54	0.46188	0.79225	1.84081	1.13175

Table B.4. Size, Shape, Pressure, and Volume of Bubbles and Drops with Given Radius of Attachment

$$r/a = 0.6$$

$\beta$	$\phi_r$	$x/b$	$z/b$	$h/a$	$V/a^3$
60.0	6.98	0.11094	0.00647	0.21801	0.01748
30.0	9.75	0.15492	0.01266	0.30724	0.02813
18.0	12.64	0.20000	0.02120	0.39692	0.03656
12.0	15.54	0.24495	0.03198	0.48658	0.04515
8.0	19.17	0.30000	0.04838	0.59676	0.05604
5.5	23.35	0.36181	0.07133	0.72131	0.06879
4.0	27.72	0.42426	0.09970	0.84811	0.08255
3.5	29.83	0.45356	0.11501	0.90807	0.08935
2.9	33.16	0.49827	0.14101	1.00025	0.10029
2.3	37.95	0.55950	0.18242	1.12813	0.11668
2.0	41.31	0.60000	0.21408	1.21407	0.12865
1.8	44.15	0.63246	0.24231	1.28397	0.13910
1.7	45.82	0.65079	0.25954	1.32394	0.14544
1.5	49.88	0.69282	0.30298	1.41709	0.16135
1.25	57.15	0.75895	0.38608	1.57014	0.19222
1.2	59.11	0.77460	0.40935	1.60808	0.20112
1.1	63.92	0.80904	0.46757	1.69516	0.22420
1.0	70.86	0.84853	0.55331	1.80546	0.26115
1.0	110.89	0.84853	0.97076	2.10065	0.61473
1.1	119.62	0.80904	1.01944	2.10444	0.74147
1.2	126.22	0.77460	1.04278	2.09873	0.85283
1.25	129.07	0.75895	1.04934	2.09449	0.90534
1.5	140.75	0.69282	1.05581	2.06906	1.14754
1.7	148.28	0.65079	1.04488	2.04798	1.32506
1.8	151.67	0.63246	1.03679	2.37679	1.40998
2.0	157.90	0.60000	1.01784	2.01784	1.57280
2.3	166.26	0.55950	0.98579	1.98964	1.80255
3.0	183.08	0.48990	0.90845	1.92912	2.28289
3.5	193.87	0.45356	0.85574	1.88796	2.58703
4.0	204.25	0.42426	0.80597	1.84692	2.86294
6.0	258.64	0.34641	0.60326	1.62222	3.68271
6.0	281.23	0.34641	0.55639	1.54104	3.59171
4.0	332.13	0.42426	0.55032	1.48537	2.56096
3.0	351.28	0.48990	0.59863	1.54966	2.03835

Table B.5. Size, Shape, Pressure, and Volume of Bubbles and Drops with Given Radius of Attachment

$$r/a = 1.0$$

$\beta$	$\phi_r$	$x/b$	$z/b$	$h/a$	$V/a^3$
60.0	13.46	0.18257	0.01914	0.28739	0.17182
30.0	19.24	0.25820	0.03877	0.40835	0.24755
18.0	25.24	0.33333	0.06585	0.53089	0.32807
16.0	26.91	0.35355	0.07454	0.56438	0.35097
12.0	31.60	0.40825	0.10137	0.65655	0.41635
8.0	40.18	0.50000	0.15888	0.81776	0.54200
6.5	45.96	0.55470	0.20262	0.91998	0.63182
5.5	51.73	0.60302	0.24929	1.01642	0.72663
4.5	61.02	0.66667	0.32813	1.15886	0.89237
4.0	69.09	0.70711	0.39734	1.26903	1.05200
3.7	77.81	0.73522	0.46919	1.37338	1.24390
3.7	103.15	0.73522	0.63176	1.59450	1.95007
4.0	113.93	0.70711	0.67052	1.65536	2.32888
4.5	125.33	0.66667	0.69002	1.70170	2.78302
5.5	140.90	0.60302	0.68546	1.73973	3.48414
6.5	152.52	0.55470	0.66411	1.75195	4.05442
8.0	166.51	0.50000	0.62550	1.75100	4.76824
10.0	181.82	0.44721	0.57493	1.73279	5.54361
16.0	220.40	0.35355	0.44901	1.62354	7.13667
20.0	253.01	0.31623	0.36935	1.48421	7.66733
20.0	286.54	0.31623	0.32147	1.33281	7.19870
16.0	316.08	0.35355	0.31169	1.23514	6.05930
10.0	348.47	0.44721	0.35006	1.22997	4.49208

Table B.6. Size, Shape, Pressure, and Volume of Bubbles and Drops with Given Radius of Attachment

$$r/a = 1.5$$

$\beta$	$\phi_r$	$x/b$	$z/b$	$h/a$	$V/a^3$
100.0	21.00	0.21213	0.03058	0.35762	0.83884
80.0	23.69	0.23717	0.03859	0.40220	0.94928
60.0	27.71	0.27386	0.05210	0.46793	1.11632
40.0	34.97	0.33541	0.08054	0.58381	1.42593
30.0	41.80	0.38730	0.11119	0.68884	1.72815
24.0	48.69	0.43301	0.14478	0.79022	2.04596
20.0	56.13	0.47434	0.18271	0.89402	2.40649
18.0	61.81	0.50000	0.21185	0.96887	2.69503
16.0	70.85	0.53033	0.25677	1.07982	3.18127
18.0	124.73	0.50000	0.39672	1.52349	6.89629
20.0	133.98	0.47434	0.39444	1.56354	7.66084
24.0	148.02	0.43301	0.38033	1.60617	8.85724
30.0	163.84	0.38730	0.35409	1.62959	10.20717
50.0	200.61	0.30000	0.27914	1.59568	12.93770
64.0	222.48	0.26517	0.23868	1.52697	13.97587
80.0	255.04	0.23717	0.19292	1.37824	14.29483
80.0	284.50	0.23717	0.16827	1.22238	13.20281
64.0	313.14	0.26517	0.16132	1.08935	11.13856
50.0	330.62	0.30000	0.16778	1.03892	9.65580
32.0	354.65	0.37500	0.19654	1.03617	7.76366

### C. COMPUTER PROGRAM

The Fortran listing of the computer program for solving the interfacial equation and computing the various parameters presented in this report is given in Table C.1. The ranges of  $\phi$ ,  $\beta$ , and  $r/a$  can be easily extended at some sacrifice of either the running time or the accuracy. Other parameters, such as maximum drop height and radius as a function of drop volume and contact angle, can be obtained either by modifying one of the MAIN subroutines or by adding another routine.

Table C.1. Computer Program

```

C SOLUTION OF INTERFACIAL EQ. FOR THE PRESS. AND VOL.
C WITHIN ATTACHED BUBBLE. CASE 1-ATTACHED ABOVE (POSITIVE BETA)
C
      IMPLICIT REAL*8 (D),REAL*4 (A-C,E-H,O-Z)
      DIMENSIONA(4),B(4),C(4),D(4),E(8),R(4),G1(10),P(4)
      DIMENSIONDA(4),DB(4),DC(4),DZ(4),DE(8),DP(4),DR(4)
      9  FORMAT (I1,I2)
      11 READ  9,I,N3
          IF (I-1)401,10,501
C
C SOLUTION AT MAX.PRESS FOR GIVEN VALUES OF R/A(=G)
C
      300 FORMAT(F15.7)
      10 CONTINUE
          DO 201 N4=1,N3
              READ300,G
C ESTIMATE OF INITIAL BETA
          IF(G.GE.0.099.AND.G.LT.0.4)GOTO1001
          IF(G.GE.0.39.AND.G.LT.0.8)GOTO1002
          IF(G.GE.0.79.AND.G.LT.3.01)GOTO1003
      1001 BETA=.11175-.92434*G+3.92521*G**2.
          GOTO301
      1002 BETA=2.87267-12.78143*G+16.40021*G**2.
          GOTO301
      1003 BETA=16.30443-49.43188*G+40.54628*G**2.
          GOTO301
C COURSE BETA GRID
      301 BETA=BETA+0.1*BETA
          N20=0
          P(2)=0
          58 BETA=BETA-.01*BETA
              CALL MAINS(A,B,C,Z,E,H,J,P,BETA,G,R)
              IF(P(1)-P(2))59,59,60
          60 P(2)=P(1)
              N20=N20+1
              GOTO58
          59 IF(N20-1)301,301,57
          57 PRINT 50,BETA,H
              PRINT 100
              PRINT 200,E(8),E(6),E(7),R(1),P(1),V
              BETA=BETA+.02*BETA
              P(2)=0
C FINE BETA GRID
          65 BETA=BETA-.001*BETA
              CALL MAINS(A,B,C,Z,E,H,J,P,BETA,G,R)
              IF(P(1)-P(2))61,61,62
          62 P(2)=P(1)
              GOTO65

```



Table C.1 (Continued)

```

61 PRINT 50,BETA,H
   PRINT 100
   PRINT 200,E(8),E(6),E(7),R(1),P(1),V
   BETA=BETA+.002*BETA
   DP(2)=0
C EXTRA FINE BETA GRID WITH DOUBLE PRECISION
   DBETA=BETA
   DG=G
66 DBETA=DBETA-.0001*DBETA
   CALL MAIND(DA,DB,DC,DZ,DE,DH,J,DP,DBETA,DG,DR)
   IF(DP(1)-DP(2))63,63,64
64 DP(2)=DP(1)
   GOTO66
63 DV=3.14159265*DG *(DP(1)*DG -DSIN(DE(5)))
   DE(4)=DE(1)*57.29577957
   DE(8)=DE(5)*57.29577957
   PRINT 50,DBETA,DH
   50 FORMAT(1H2,6HBETA =,E15.7,6X,3HH =,E15.7///)
100 FORMAT(1H0,5X,3HPHI,8X,3HX/B,13X,3HZ/B,13X,3HR/A,13X,3HH/A,
113X,4HV/A3)
200 FORMAT(1H ,OP1F9.3,1P5E16.7)
   PRINT100
   PRINT200,DE(8),DE(6),DE(7),DG,DP(1),DV
201 CONTINUE
   GOTO 11
C
C SOLUTION FOR GIVEN VALUES OF BETA AND R/A(=G1)
C
400 FORMAT(8F10.7)
401 CONTINUE
   DO 202 N4=1,N3
   READ 400,BETA,(G1(I),I=1,8)
   CALL MAINIS(A,B,C,Z,E,H,J,P,BETA,G1,R)
202 CONTINUE
   GOTO 11
C
C SOLUTION FOR GIVEN VALUES OF BETA AT INTERVALS (N1) OF PHI
C                                     UP TO N2
501 CONTINUE
   DO 203 N4=1,N3
   READ 500,BETA,N1,N2
500 FORMAT(F10.7,2I4)
   CALL MAIN2S(A,B,C,Z,E,H,J,P,BETA,G,R,N1,N2)
203 CONTINUE
   GOTO 11
   END
C
C
C

```

Table C.1 (Continued)

---

```

SUBROUTINE MAINS(A,B,C,Z,E,H,J,P,BETA,G,R)
C
  IMPLICIT REAL*8(D),REAL*4(A-C,E-H,O-Z)
  DIMENSION A(4),B(4),C(4),Z(4),E(8),P(4),R(4)
  H=0.1745329E-01
  E(6)=0.
  J=3
  E(1)=0.
  E(2)=0.
  E(3)=0.
  N1=1
  R(2)=0.
  DO150M=1,360
  CALL RUNGKS(A,B,C,Z,E,H,J,BETA,G,P)
  R(1)=E(2)*SQRT(BETA/2.0)
  GOTO(4,5),N1
  4 IF(G-R(1))5,3,3
  3 IF(R(1)-R(2))8,8,10
  5 IF(G-R(1))1,6,7
  1 N1=2
  10 R(2)=R(1)
  E(5)=E(1)
  E(6)=E(2)
  E(7)=E(3)
  150 CONTINUE
  7 F=(G-R(2))/(R(1)-R(2))
  E(5)=F*(E(1)-E(5))+E(5)
  E(6)=F*(E(2)-E(6))+E(6)
  E(7)=F*(E(3)-E(7))+E(7)
  6 P(1)=SQRT(2./BETA)+E(7)*SQRT(BETA/2.)
  GOTO9
  8 P(1)=1.0
  P(2)=2.0
  9 RETURN
  END
C
C
C
C
SUBROUTINE MAIND(DA,DB,DC,DZ,DE,DH,J,DP,DBETA,DG,DR)
C
  IMPLICIT REAL*8(D),REAL*4(A-C,E-H,O-Z)
  DIMENSION DA(4),DB(4),DC(4),DZ(4),DE(8),DP(4),DR(4)
  DH=0.8726646D-02
  DE(6)=0.
  J=3
  DE(1)=0.
  DE(2)=0.
  DE(3)=0.
  N1=1

```

Table C.1 (Continued)

```

DO150M=1,720
CALL RUNGKD(DA,DB,DC,DZ,DE,DH,J,DBETA,DG,DP)
DR(1)=DE(2)*DSQRT(DBETA/2.0)
GOTO(4,5),N1
4 IF(DG-DR(1))5,150,150
5 IF(DG-DR(1))1,6,7
1 DR(2)=DR(1)
DE(5)=DE(1)
DE(6)=DE(2)
DE(7)=DE(3)
N1=2
150 CONTINUE
7 DF=(DG-DR(2))/(DR(1)-DR(2))
DE(5)=DF*(DE(1)-DE(5))+DE(5)
DE(6)=DF*(DE(2)-DE(6))+DE(6)
DE(7)=DF*(DE(3)-DE(7))+DE(7)
6 DP(1)=DSQRT(2./DBETA)+DE(7)*DSQRT(DBETA/2.)
RETURN
END
C
C
C
C
SUBROUTINE MAINIS(A,B,C,Z,E,H,J,P,BETA,G1,R)
IMPLICIT REAL*8(D),REAL*4(A-C,E-H,O-Z)
DIMENSIONA(4),B(4),C(4),Z(4),E(8),P(4),R(4),G1(10)
H=0.8726646E-02
E(6)=0.
J=3
R(2)=0.
E(1)=0.
E(2)=0.
E(3)=0.
N2=1
N1 = 1
I=1
DO 150 M=1,720
CALL RUNGKS(A,B,C,Z,E,H,J,BETA,G1,P)
R(1)=E(2)*SQRT(BETA/2.0)
GOTO(4,5,22),N1
4 IF(G1(I)-R(1))7,6,3
3 IF(R(1)-R(2))10,10,140
10 I=I-1
5 N2=-1
N1=2
IF(G1(I)-R(1))20,6,7
20 IF(R(1)-R(2))140,21,21
21 I=I+1

```

Table C.1 (Continued)

```

22 N2=1
    N1=3
    IF(G1(I)-R(1))7,6,140
 7 F=(G1(I)-R(2))/(R(1)-R(2))
    E(1)=F*(E(1)-E(5))+E(5)
    E(2)=F*(E(2)-E(6))+E(6)
    E(3)=F*(E(3)-E(7))+E(7)
 6 P(1)=SQRT(2./BETA)+E(3)*SQRT(BETA/2.)
    V=3.14159265*G1(I)*(P(1)*G1(I)-SIN(E(1)))
    E(4)=E(1)*57.29577957
50 FORMAT(1H2,6HBETA =,E15.7,6X,3HH =,E15.7///)
    PRINT 50,BETA,H
    PRINT 100
    PRINT 200,E(4),E(2),E(3),G1(I),P(1),V
200 FORMAT(1H ,OP1F9.3,1P5E16.7)
100 FORMAT(1H0,5X,3HPHI,8X,3HX/B,13X,3HZ/B,13X,3HR/A,13X,3HH/A,
 113X,4HV/A3)
    I=I+N2
    IF(I-8)130,130,3
130 IF(I-1)9,140,140
140 R(2)=R(1)
    E(5)=E(1)
    E(6)=E(2)
    E(7)=E(3)
150 CONTINUE
 9 RETURN
    END
C
C
C
C
SUBROUTINE MAIN2S(A,B,C,Z,E,H,J,P,BETA,G,R,N1,N2)
    IMPLICIT REAL*8(D),REAL*4(A-C,E-H,O-Z)
    DIMENSION A(4),B(4),C(4),Z(4),E(8),P(4),R(4)
101 FORMAT(1H0,5X,3HPHI,8X,3HX/B,13X,3HZ/B,13X,3HR/A,13X,3HH/A,
 113X,4HV/A3)
 50 FORMAT(1H1,5HBETA=,E15.7,6X,2HH=,E15.7///)
200 FORMAT(1H ,OP1F9.3,1P5E16.7)
    H=0.1745329E-01
    PRINT 50,BETA,H
    PRINT 101
    E(6)=0.
    J=3
    N2=N2/N1
    N3=.1746E-01/H
    N1=N3*N1
    E(1)=0.
    E(2)=0.
    E(3)=0.
    DO 150 M=1,N2

```

Table C.1 (Continued)

```

DO 100 N=1,N1
CALL RUNGKS(A,B,C,Z,E,H,J,BETA,G,P)
100 CONTINUE
G=E(2)*SQRT(BETA/2.0)
E(6)=E(2)
E(7)=E(3)
P(1)=SQRT(2./BETA)+E(7)*SQRT(BETA/2.)
V=3.141593*G*(P(1)*G-SIN(E(1)))
E(4)=E(1)*57.29577957
PRINT 200,E(4),E(6),E(7),G,P(1),V
150 CONTINUE
RETURN
END

```

C  
C  
C

```

SUBROUTINE RUNGKD(DA,DB,DC,DZ,DE,DH,J,DBETA,DG,DP)

```

C

```

IMPLICIT REAL*8(D),REAL*4(A-C,E-H,O-Z)
DIMENSION DA(4),DB(4),DC(4),DZ(4),DE(8),DP(4),DR(4)
DA(1)=DH*0.166666666667
DA(2)=DH*0.333333333333
DA(3)=DA(2)
DA(4)=DA(1)
DB(4)=0.
DB(1)=DH*0.5
DB(2)=DB(1)
DB(3)=DH
DO20 I=1,J
DC(I)=0.
20 DZ(I)=DE(I)
DO30 K=1,4
CALL RHOD(DA,DB,DC,DZ,DE,DH,J,DBETA,DG,DP)
DZ(1)=1.
DO50 I=1,J
DC(I)=DC(I)+DA(K)*DZ(I)
50 DZ(I)=DE(I)+DB(K)*DZ(I)
30 CONTINUE
DC(1)=DH
DO60 I=1,J
60 DE(I)=DE(I)+DC(I)
RETURN
END

```

C  
C  
C

```

SUBROUTINE RHOD(DA,DB,DC,DZ,DE,DH,J,DBETA,DG,DP)

```

C

```

IMPLICIT REAL*8(D),REAL*4(A-C,E-H,O-Z)
DIMENSION DA(4),DB(4),DC(4),DZ(4),DE(8),DP(4),DR(4)

```

Table C.1 (Continued)

```

IF(DZ(1))70,75,70
70 DRH=1.0/(2.0+DBETA*DZ(3)-DSIN(DZ(1))/DZ(2))
   GOTO76
75 DRH=1.0
76 DZ(2)=DRH*DCOS(DZ(1))
   DZ(3)=DRH*DSIN(DZ(1))
   RETURN
   END
C
C
C
SUBROUTINERUNGKS(A,B,C,Z,E,H,J,BETA,G,P)
C
IMPLICIT REAL*8(D),REAL*4(A-C,E-H,O-Z)
DIMENSIONA(4),B(4),C(4),Z(4),E(8),P(4),R(4)
A(1)=H*0.166666666667
A(2)=H*0.333333333333
A(3)=A(2)
A(4)=A(1)
B(4)=0.
B(1)=H*0.5
B(2)=B(1)
B(3)=H
DO20I=1,J
C(I)=0.
20 Z(I)=E(I)
   DO30K=1,4
   CALLRHOS(A,B,C,Z,E,H,J,BETA,G,P)
   Z(1)=1.
   DO50I=1,J
   C(I)=C(I)+A(K)*Z(I)
50 Z(I)=E(I)+B(K)*Z(I)
30 CONTINUE
   C(1)=H
   DO60I=1,J
60 E(I)=E(I)+C(I)
   RETURN
   END
C
C
C
SUBROUTINERHOS(A,B,C,Z,E,H,J,BETA,G,P)
C
IMPLICIT REAL*8(D),REAL*4(A-C,E-H,O-Z)
DIMENSIONA(4),B(4),C(4),Z(4),E(8),P(4),R(4)
IF(Z(1))70,75,70
70 RH=1.0/(2.0+BETA*Z(3)-SIN(Z(1))/Z(2))
   GOTO76
75 RH=1.0
76 Z(2)=RH*COS(Z(1))
   Z(3)=RH*SIN(Z(1))
   RETURN
   END

```

## INTERNAL DISTRIBUTION

1. G. G. Alexander
2. N. G. Anderson
3. C. F. Baes
4. C. J. Barton
5. M. S. Bautista
6. S. E. Beall
7. E. S. Bettis
8. F. F. Blankenship
9. G. E. Boyd
10. J. Braustein
11. M. A. Bredig
12. R. B. Briggs
13. H. R. Bronstein
14. R. D. Bundy, K-25
15. S. Cantor
16. R. H. Chapman
17. S. J. Claiborne, Jr.
18. E. L. Compere
- 19-28. J. W. Cooke
29. W. B. Cottrell
30. J. L. Crowley
31. F. L. Culler
32. J. H. DeVan
33. A. S. Dworkin
34. D. M. Eissenberg
35. A. P. Fraas
36. D. E. Ferguson
37. M. H. Fontana
38. H. A. Freidman
39. W. K. Furlong
40. C. H. Gabbard
41. R. B. Gallaher
42. W. R. Gambill
43. L. O. Gilpatrick
44. W. R. Grimes
45. A. G. Grindell
46. W. O. Harms
47. P. N. Haubenreich
48. B. F. Hitch
- 49-50. H. W. Hoffman
51. C. C. Hurtt
52. P. R. Kasten
53. R. J. Kedl
54. J. J. Keyes, Jr.
55. G. J. Kidd, Jr., K-25
56. S. S. Kirsulis
57. O. H. Klepper
58. J. W. Koger
59. J. O. Kolb
60. R. B. Korsmeyer
61. A. I. Krakoviak
62. T. S. Kress
63. J. W. Krewson
64. M. E. Lackey
65. M. E. LaVerne
66. C. G. Lawson
67. G. H. Llewellyn
68. D. B. Lloyd
69. M. I. Lundin
70. R. N. Lyon
71. R. E. MacPherson
72. T. H. Mauney
73. H. C. McCurdy
74. D. L. McElroy
75. H. A. McLain
76. L. E. McNeese
77. J. R. McWherter
78. A. J. Miller
79. W. R. Mixon
80. R. L. Moore
81. L. F. Parsley
82. A. M. Perry
83. J. Pidkowicz
84. J. D. Redmon
85. D. M. Richardson
86. G. D. Robbins
87. K. A. Romberger
88. M. W. Rosenthal
89. R. G. Ross
90. G. Samuels
91. J. P. Sanders
92. W. K. Sartory
93. H. C. Savage
94. Dunlap Scott
95. J. H. Shaffer
96. Myrtlelen Sheldon
97. J. D. Sheppard
98. M. J. Skinner
99. I. Spiewak
100. D. A. Sunberg
101. R. E. Thoma
102. D. G. Thomas
103. D. B. Trauger
104. M. L. Tobias
105. J. L. Wantland
106. J. S. Watson
107. C. F. Weaver
108. G. D. Whitman
109. R. P. Wichner
110. M. M. Yarosh

- 111. J. P. Young
- 112. H. C. Young
- 113-114. Central Research Library
- 115. Y-12 Document Research Section
- 116-117. Laboratory Records
- 118. Laboratory Records - Record Copy

## EXTERNAL DISTRIBUTION

- 119-121. Director, Division of Reactor Licensing, AEC, Washington
- 122-123. Director, Division of Reactor Standards, AEC, Washington
- 124-125. Division of Technical Information Extension (DTIE)
- 126. Laboratory and University Division, AEC, ORO
- 127. D. F. Cope, RDT Site Office, ORNL
- 128. A. R. DeGrazia, AEC, Washington
- 129. Ronald Feit, AEC, Washington
- 130. Norton Haberman, AEC, Washington
- 131. Kermit Laughon, RDT Site Office, ORNL
- 132-133. T. W. McIntosh, AEC, Washington
- 134. R. M. Scroggins, AEC, Washington
- 135-139. Executive Secretary, Advisory Committee on Reactor Safeguards, AEC, Washington